Response to reviewers for "**Characterization of Ozone Production in San Antonio, Texas Using Measurements of Total Peroxy Radicals".**

We thank both reviewers for their helpful comments. Responses to the individual comments are shown below in red. Line numbers in red refer to the revised submission that does not include tracked changes.

Anonymous Referee #1

General Comments

The manuscript analyzes total peroxy radical observations made by the Ethane Chemical AMPlifier (ECHAMP) in addition to coincident air chemistry measurements aboard the Aerodyne Mobile Laboratory during May 2017 in the vicinity of San Antonio, TX. The authors characterize the gross ozone production rate (P(O3)) and the total peroxy radical production rate, NOx-VOC sensitivity to P(O3), and species contributing to OH reactivity in this region. Mechanisms driving ozone levels in San Antonio, TX were postulated based on upwind measurement sites, as well as other routine measurement sites within the Texas Commission for Environmental Quality monitoring network. The authors present a cohesive analysis of P(O3) in the San Antonio study areas, based on the ECHAMP and accompanying Aerodyne Mobile Laboratory measurements, using model analyses and satellite retrievals to support claims made relating to ozone production sensitivity to NOx within this region, with less ozone produced here than in Houston, TX. The authors also find that the main drivers of afternoon OH reactivity are primarily biogenic, in contrast to previous field studies in the area. Publication of this manuscript is recommended after the following points have been addressed.

Specific Comments:
Lines 156-163: Some of the major conclusions with respect to OHR are drawn from the PTR isoprene measurements, and while these conclusions relating to the species dominating OHR are unchanged given the calculated isoprene uncertainty, more information is needed to convince readers of the robustness of this measurement and efforts made to appropriately scale the PTR isoprene measurements. In particular, SI Line 207 indicates that the PTR isoprene sensitivity was scaled to the sensitivity in GC isoprene plus six additional hydrocarbons. Which other hydrocarbons were measured and why not directly compare the isoprene sensitivities to each other? Some additional explanation here is needed either in the main text or the SI, perhaps along with a figure of the direct isoprene PTR-GC sensitivity comparisons in addition to the summed PTR-GC sensitivity comparisons.

We were not adequately clear in our description of how we arrived at the isoprene sensitivity for the AQRP campaign. There was no isoprene standard available during the SAFS field deployment for the GC, so the isoprene sensitivity for the GC was not determined in the field. A multi-component standard containing isoprene and six other hydrocarbons measured during AQRP (iso-pentane, *n*-pentane, *n*-hexane, methylcylcopentane, cyclohexane, and benzene) was available during a later campaign, in which the GC had a slightly different setup. The isoprene sensitivity for this configuration was determined, but since the configuration differed from SAFS, this sensitivity could not be directly applied to the data obtained in San Antonio. Instead, the sensitivities of the other six hydrocarbons that were present in standards available at both campaigns were compared. Overall, the mean ratio of sensitivities from SAFS to the second campaign for these six gases was 0.34. So, to determine the isoprene sensitivity for SAFS, the sensitivity for the second campaign was determined by dividing this value by 0.34.

We have updated the wording in the SI to try to make this clearer. We have also included a figure comparing the GC isoprene sensitivity, determined by the method described above, with the PTR sensitivity determined in the field. These are the only two isoprene values available from the campaign so are the only values we could compare. In addition, we now compare the scaled PTR isoprene to observations made by TCEQ at their Floresville monitoring site, which was co-located with the AML.

The isoprene section now reads (Lines 204 – 231 in the SI):

> "No isoprene standard was available during SAFS for online calibration of the GC-MS observations, so an isoprene sensitivity was not determined during the campaign. Approximately 6-months after SAFS, a calibration of the same instrument was conducted during a second campaign using a multi-component mixture, including isoprene and 6 other hydrocarbons (iso-pentane, *n*-pentane, *n*-hexane, methylcyclopentane, cyclohexane, and benzene) measured during SAFS. To determine a sensitivity for isoprene for SAFS, the sensitivities for the six hydrocarbons during SAFS was compared to that for the second campaign, in which the GC setup differed in both sample trap temperature and detector micro channel plate voltage from the SAFS configuration. The mean ratio of sensitivities from SAFS to the second campaign for the six overlapping hydrocarbons was 0.34 ± 0.10 (1σ), while the slope of a regression line of the SAFS sensitivities to the second campaign sensitivities was 0.38. The isoprene sensitivity for SAFS was then determined by dividing the sensitivity to isoprene at the second campaign by the average of these two values (0.36). The total uncertainty (1σ) in the isoprene observations is estimated as 31%, with the sensitivity uncertainty dominating.
>
> While there was an in-field calibration for the PTR derived isoprene, it was determined that the isoprene concentration in this older calibration tank was most likely lower than the stated value, biasing the PTR results. There were overlapping observations of the PTR and GC derived isoprene values from the start of the campaign to 19 May, after which the GC trap was damaged. So that we have calibrated isoprene observations for the duration of the campaign, we have scaled the PTR derived isoprene to GC values for this overlapping period. The 1-minute averaged PTR data were averaged to the GC sampling time, and a linear least squares regression was used to determine the relationship. This resulted in a fit with an r^2 of 0.91 and a relationship between the two instruments as follows: $[C_5H_8]_{GC} = 0.787[C_5H_8]_{PTR} - 0.15$ (Fig. S7). The normalized mean bias for this relationship was 7%.
>
> To evaluate the scaled PTR isoprene, we compare these values to isoprene measurements made hourly by a GC at the Floresville TCEQ site. The scaled PTR isoprene was averaged to the TCEQ sampling frequency and regressed against the TCEQ isoprene. This yielded a slope of 0.93 with an r^2 of 0.88. There was an offset of 0.10 ppbv between the two data sets with the TCEQ isoprene higher. The excellent agreement between the scaled PTR isoprene and the TCEQ isoprene further validates the isoprene results presented here."

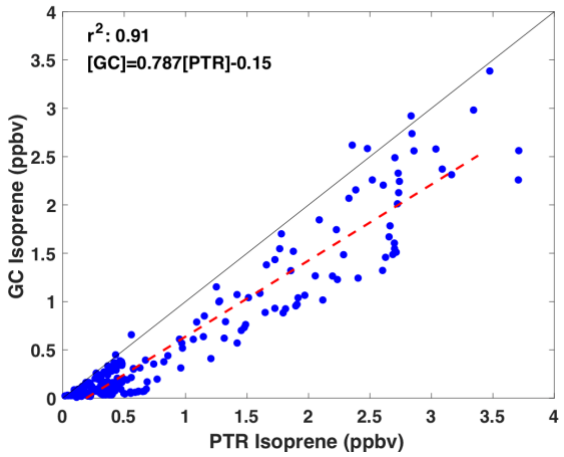

Figure S7: Comparison of isoprene measured by the PTR to observations from the GC. The isoprene sensitivity of the GC was determined several months after the campaign as described in the text.

Section 2.2: While a full description of the ECHAMP measurement can be found in Wood (2017), it would be useful for the reader if the authors very briefly describe the ECHAMP methodology in a few sentences at the beginning of this section.

We have added the following summary of the ECHAMP instrument to lines 182 – 189 in section 2.2.

> "Briefly, ECHAMP measures total XO_2 concentration at a two-minute resolution by reacting peroxy radicals with excess NO and ethane (C_2H_6). Through a series of chain reactions, each XO_2 radical produces approximately 20 NO_2 molecules (depending on the relative humidity (RH)), which are then measured with a commercially available NO_2 monitor. Because this NO_2 monitor also measures ambient O_3 and NO_2 (O_X), a second channel and dedicated NO_2 monitor are used to only measure the sum of [O_3] and [NO_2]. The difference between the two channels, divided by the "amplification factor" of ~20, yields the XO_2 concentration."

Section 2.3 – The calculation of gross P(O3) is presented here, but the authors have measured the majority of the main constituents needed to calculate net P(O3). Thus, P(O3) presented here is presumably overestimated (even if only slightly). I would recommend that, for completeness, the authors calculate net P(O3) as in Sommariva et al., 2011. An estimate of the uncertainty in this calculated P(O3) is also needed.

We have presented values for gross $P(O_3)$ in lieu of net $P(O_3)$ so that the calculated values can be tied directly to observations. Calculating net $P(O_3)$ requires knowledge of both OH and the fraction of total XO_2 comprised of HO_2, neither of which were observed during the campaign.

We have added the following discussion to the text (Lines 265 – 282):

> "The net formation rate of O_3 is equal to $P(O_3)_{Gross} - L(O_3)$. In order to tie $P(O_3)$ completely to observations, we report only gross $P(O_3)$, not net $P(O_3)$. That is, we only calculate the production term (Eq. 2) and not the loss term (Eq. 4) for net ozone production. Calculation of the loss term requires knowledge of the concentration of OH and alkenes as well as the fraction of total XO_2 comprised of HO_2, none of which were measured during SAFS. Alkene concentrations, except for isoprene and monoterpenes, were not measured during

SAFS. Estimating the alkene loss term using concentrations from nearby TCEQ monitoring sites, suggests that O_3 loss due to this pathway is negligible for the data analyzed here, and we omit this from our calculation of ozone loss. To estimate OH and the fraction of XO_2 comprised of HO_2 and to determine whether analyzing only gross $P(O_3)$ affects our conclusions, we used the Framework for 0-Dimensional Atmospheric Modeling (F0AM) box model (Wolfe et al., 2016b) to calculate OH and the fraction of RO_2 comprised of HO_2. A description of the model setup can be found in the SI. For data points that were not modeled due to missing model constraints, these values were estimated from interpolation of modeled values, if observations were made within two hours of a modeled data point, or from site-specific mean daily profiles if no modeled points were available. Using these modeled-derived values for OH and the HO_2 fraction, median $L(O_3)$ for daytime observations at all sites were determined to be 0.90 ppbv/hr, which is 16% of the gross production rate."

We estimate total uncertainty in the gross ozone production rate as 34%, and we described this in the text as follows (Lines 252 – 263);

"At 298 K, k_{NO+HO2} is within 10% of the k values for the reaction of NO with CH_3O_2 and isoprene RO_2 (Orlando and Tyndall, 2012), supporting our choice of k_{eff}. Further, while the reaction of NO with acetyl peroxy radicals is approximately 2.5 times faster than with other peroxy radicals at 298K, box modeling results suggest that these radicals comprise only 5 – 10% of total XO_2, resulting in an average difference in $P(O_3)$ of 15% from the k_{NO+HO2} value used here. This uncertainty is comparable to the total uncertainty of the k_{NO+HO2} rate constant, estimated as 15% (Sanders et al., 2011). As will be shown in Section 3.2, our conclusions are insensitive to the value of k_{eff} chosen. Uncertainty in gross $P(O_3)$ results from uncertainty in the NO and XO_2 measurements, 5% and 25%, respectively, and k_{eff}, whose uncertainty we estimate at 23%, determined by adding the uncertainty in the k_{NO+HO2} rate constant and the uncertainty in the choice of k_{eff} in quadrature. This results in a total $P(O_3)$ uncertainty of 34%."

Lines 406-408: More clarification is needed to discuss how the contribution of alkenes to OHR was determined. Presumably, the contribution was determined from adding the alkenes measured at TCEQ sites nearest UTSA and Floresville to the observed mobile laboratory hydrocarbon mixtures at UTSA and Floresville to approximate the difference in OHR, but it is unclear in the text. Another sentence or two here could help to clarify.

We agree that the wording describing the estimation of alkene concentrations was confusing. We have expanded this discussion into its own paragraph at the end of the OH reactivity section (Lines 505 – 524) in the revised text:

"Because of the large contribution of alkenes to OH reactivity at other Texas sites (Mao et al., 2010), it is necessary to make an estimate of their importance during SAFS. With the exception of isoprene and monoterpenes, alkenes were not measured onboard the AML and therefore have not been included in the above analysis. To estimate the impact of anthropogenic alkenes on OH reactivity, we include in our calculation of OH reactivity observations of alkenes made at nearby TCEQ monitoring sites, Camp Bullis for UTSA and a site in Floresville co-located with the AML. These sites provide hourly observations of cis-2-butene, trans-2-butene, 1-pentene, cis-2-pentene, trans-2-pentene, ethene, propene, 1,3-butadiene, and 1-butene. Alkene concentrations at the SAFS monitoring sites were assumed to be identical to those at the TCEQ monitoring sites and were interpolated to the

ECHAMP time base. This assumption is likely more accurate for the Floresville site than for UTSA. A regression of hourly averaged *n*-pentane measured onboard the AML to that measured at the Camp Bullis TCEQ site has an r^2 of 0.3, even after maximizing the correlation using a lead-lag analysis. In addition, the maximum *n*-pentane concentrations at the Camp Bullis site are almost a factor of 2 higher than those seen at UTSA. Regressions of cyclohexane and benzene between the two sites show even lower r^2 values. On the other hand, a similar regression of n-pentane at the Floresville site has an r^2 of 0.83. Better agreement at Floresville is to be expected since the AML and TCEQ monitor were co-located. Total OH reactivity was then recalculated using the estimates of alkene concentrations. Alkenes contribute less than 1% of total reactivity at both UTSA and Floresville for morning and afternoon times."

Are there differences in total XO2 measured and total XO2 modeled that would indicate missing OHR, potentially from alkenes?

This is a good point and is one that we have started to investigate. Preliminary box modeling results using multiple chemical mechanisms overestimate observed XO_2 by 0 to 30%, well within the combined measurement and modeling uncertainty. This would suggest that no additional VOCs, including alkenes, are needed to explain the observed XO_2 and that the OH reactivity reported here is also accurate. We choose not to present those results here, however, because we plan on publishing a separate publication on model results in the coming months. Inclusion of modeling results in this paper, beyond that used for the L_n/Q analysis, would expand the scope of this paper too much, resulting in a paper of unwieldy length.

Section 4, Lines 448-453: The discussion of ozone production and potential formation mechanisms could be expanded upon more in the discussion. It seems that, instead of hypothesizing the cause of differences between upwind and downwind San Antonio sites, one could examine the change in ozone with time in comparison to calculated P(O3) to evaluate whether these areas experience locally-produced versus advected ozone. In the above-mentioned lines, southeasterly winds would seem consistent with the lower Calaveras Lake O3 and higher UTSA measured O3, supporting an urban source or in situ production in the urban outflow. However, there is no mention of the prevailing wind direction before May 17th when the Calaveras Lake O3 agrees quite well with the UTSA O3. Could winds or back trajectories provide any clue to further substantiate causes for the observed ozone levels downwind of the urban core? Finally, there is no mention of the Pecan Valley O3 in Fig. S3 or in the discussion, begging the question of whether or not this measurement site provides additional evidence for the observed O3 patterns in this area.

We have added the time series of ozone observations at Pecan Value to Figure S5 (formally Figure S3) and discuss these observations in lines 574 – 577. In particular, we note that on several occasions ozone is lower at the Pecan Valley site than at either Lake Calaveras or at UTSA. This is in line with the idea that there is potentially more ozone titration in the downtown area of San Antonio, and that ozone production rates are not constant across the city.

We agree that an investigation into the evolution of ozone in an air parcel over time warrants further investigation. Future papers using both Eulerian and Lagrangian modeling are going to further investigate this topic, so we do not want to discuss this more fully here. Further, we are reluctant to include further discussion on the topic in this paper because the observations needed to determine $P(O_3)$ at all sites are unavailable. As the comparison between ozone concentrations at Lake Calaveras, Pecan Valley, and UTSA show, it is highly likely that ozone production rates are not constant across the region,

so a simple analysis of multiplying ozone production rates by the amount of time it takes to travel from one site to the other will likely not yield accurate results.

Technical Comments:
All acronyms throughout the manuscript should be defined, including chemical species formulae. In addition, the 'x' in Ox and NOx should appear as a subscript.

All instances of NO_X and O_X are now presented with the "X" as a subscript. We note that we use a capital "X" for this, that when subscripted, can be mistaken for a lower case "x".

Line 27: Define NO and NO2, as well as other chemical species formulae that are used throughout the manuscript.

We have defined these species in the revision.

Lines 43-47: Define chemical species, including O3

These species are now defined. We define O_3 in line 27 since that is the first usage of the species in the main body of the text.

Line 67: A definition of OH reactivity may be needed here as a precursor for subsequent Discussion

We have moved the definition of OH reactivity from section 3.3 to here. See lines 72 – 73.

Line 91: should be ": : :radicals (XO2 = RO2 + HO2) from three sites in the San Antonio area, characterizing the XO2 distribution in the region."

We have made this change. Now lines 94 – 95.

Line 111-112: To clarify your definition of background for this study, it should be defined here as 'upwind of the UTSA site'.

We have made this change. See lines 117 – 118.

Lines 143-155: A short description of the uncertainties in the GC/PTR observations is needed here.

In reference to the uncertainty of the PTR observations, on Lines 154-155, we now say "Typical measurement uncertainties were on the order of 25%." And for the GC observation uncertainties, we now say on Lines 160-163 "While toluene and *m*- and *p*- xylene measurement uncertainty was on the order of 20%, typical measurement uncertainties of other observed species, except isoprene, were on the order of 10%."

Line 162: Please denote that the 30% estimated uncertainty is 1 sigma.

We have indicated that the uncertainty is 1 sigma. Line 169.

Lines 181-182: The flow rates used here are inconsistent with Fig. S1.

We have updated Fig. S1 with the correct flow rates.

Line 195: Should be ‘At 15.2 cm downstream : : :”

We have made this change (now Line 209).

Line 317: ‘fresher’ should be replaced with ‘recently-emitted’

We have made this change (now Line 357).

Line 331: ‘panel a’ should be replaced with ‘panel 6a’ for clarity

We have made this change (now Line 371).

Line 345: The claim that P(O3) can be VOC-limited at NO > 200 pptv is hard to discern from Fig. 6 due to the variability in P(O3) at lower P(ROx).

In response to comments by the other reviewer, we now show an additional panel to figure 6 with the data further separated by VOC reactivity. This more clearly shows the peak associated with the transition from NO_x- to VOC-limited chemistry.

Line 392-393: To clarify, “The OH reactivity is defined as the sum of the production of the OH reaction rate coefficient for a particular species: : :”

We have made this change, although we now define OH reactivity on Lines 72 – 73.

Line 405: Can the authors quantify ‘marginal agreement’?

We have updated the text to show that a regression of observed n-pentane at UTSA and the Camp Bullis site only has an r^2 of 0.3. This is in contrast to the AML and TCEQ observations, co-located at Floresville which have an r^2 greater than 0.8. (Lines 515 – 521)

Line 427: Can authors quantify the alkane contribution at the UTSA site?

The paper now reads (Lines 495 – 497):

> “Contributions from alkanes were unimportant at the UTSA site, 1% or less during both morning and afternoon, and contributed only 4-5% at Floresville.”

Fig. 2b: White lettering of the measurement locations are difficult to see; I would recommend changes these colors to something more visible.

The labeling for the measuring locations is now yellow with a black outline.

Fig. 3: P(O3) upper quantities are cut off; consider either averaging the P(O3) signal more, or enlarging the y-axis.

We have made this change.

Fig. 7: Blue dots are difficult to see; the authors may consider fitting a line to these points.

We have increased the size of the points to make them more visible and to better distinguish these points from the Ln/Q values.

Fig S2: The caption is inconsistent with the legends in the figures

We have added the panel labels to the figure, and changed RO_2 to XO_2 and $P(HO_X)$ to $P(RO_X)$ to match the figure.

Anonymous Reviewer #2

The paper "Characterization of Ozone Production in San Antonio, Texas Using Observations of Total Peroxy Radicals" by Anderson et al. presents observations of total peroxy radicals and supporting measurements at three different sites in San Antonio, TX. The dataset is used to calculate the production rate of ozone and to provide information on the drivers of ozone formation in the area. The manuscript is well written and presented and I recommend after some modifications and clarifications.
Main Comments ————-

The measurements were made at three sites, but most of the discussion seems to be focused on the UTSA site or on aggregated data. The authors do not really use the dataset to explore the geographical differences between the three sites and what could be the underlying causes of these differences. On page 22 for example it is mentioned almost in passing that the VOC profile at the Floresville site is different (less isoprene). Does that change the main conclusions of the paper? Please add more discussion on the other sites.

We have changed the wording in the final paragraph to indicate that, while the absolute concentration of isoprene was lower at Floresville than at UTSA, it was still the dominant contributor to total OH reactivity. Because of the lower isoprene concentration, however, the total OH reactivity is about a factor of 3 lower at Floresville than at UTSA. The final paragraph (Lines 592 – 607) now reads:

> "While the isoprene concentration at Floresville was significantly lower than at UTSA, it was still the dominant contributor to OH reactivity during the afternoon, although the total OH reactivity was a factor of 3 lower at this site (4 s^{-1}) than at UTSA. Schade and Roest (2016) found a significantly different OH reactivity profile at Floresville than described here, with alkanes accounting for approximately 70% of total OH reactivity, with biogenic VOCs contributing less than 5%. Observed isoprene at Floresville during SAFS was more than an order of magnitude larger than that reported in Schade and Roest (2016), with alkane concentrations consistent between the two studies. When the data used in Schade and Roest (2016) are subset to afternoon times and May through July, the contribution of isoprene to VOC reactivity increases to a median value of 38%, in agreement with the results presented here (Schade, personal communication). The differences between the two studies do suggest that there could be significant seasonal and diurnal variations in OH reactivity. Nevertheless, these results suggest that policies designed to limit O_3 production at the SAFS sites discussed here should initially focus primarily on NO_X reductions as the region is NO_X limited and the primary VOC contributor is biogenic. Further observations and analysis are need to determine whether this holds true in the urban core of downtown San Antonio."

We now also note that the relationship between $P(O_3)$ and NO is consistent among all three sites. They differ in that $P(RO_X)$ and VOC reactivity are significantly lower at Floresville and Corpus than at UTSA, so that ozone production is significantly lower at these sites (Lines 559 – 562).

> "The relationship between $P(O_3)$ and NO was consistent at the three sites, although the lower $P(RO_X)$, NO, and VOC reactivity at Floresville and Corpus Christi led to overall lower ozone production rates as compared to UTSA."

The P(O3) values derived from this dataset are lower than those derived from observations in other areas of Texas, namely Houston. It would be interesting to have a more detailed comparison with the other datasets. Only TRAMP2006 is compared with SAFS (on page 22). Especially the TEXAQS 2006 data (Sommariva et al, 2011) which were obtained with a similar technique could be interesting to compare. Are the differences simply a matter of different VOC emissions? In addition, can you comment on the source of isoprene? If isoprene is dominant at the UTSA site but not at the other sites, do the conclusions of the study regarding NOx-limited conditions in the city still apply?

We have added a paragraph (Lines 530 – 535) comparing our results to those found during DISCOVER-AQ in 2013 in Houston. Near surface $P(O_3)$ had a median value of about 10 ppbv/hr, slightly more than a factor of 2 higher than what was seen at UTSA and a factor of 10 higher than at Floresville and Corpus. While it is difficult from the results published in Mazzuca et al to make a direct comparison to our study, both NO and $P(HO_X)$ were frequently higher in Houston than in San Antonio. Both of these could explain the higher ozone production rates. We do not compare our results directly to Sommariva, et al. because, as they note in their paper, they frequently sampled individual plumes that were not representative of the overall photochemical environment. This is quite evident when comparing the means and medians of ozone production rates at individual sites in Sommariva. We do note that the median rates observed in Sommariva are reasonably in line with Mazzuca. We refrain from making further comparisons because many of the campaigns were conducted more than a decade previous to SAFS, so both emission sources and strength have likely changed at both sites. The new paragraph reads:

> "We have presented observations of O_3, its precursors, and total observations of XO_2 at three sites in the San Antonio region. We also presented determinations of $P(O_3)$ calculated from measurements of total peroxy radicals. Median daytime $P(O_3)$ at UTSA was 4.1 ppbv/hr, compared to just over 1 ppbv/hr at the other two SAFS sites. Ozone production rates at UTSA were still far lower, however, than values observed during campaigns in Houston. Mazzuca et al. (2016) found median near surface gross $P(O_3)$ of about 10 ppbv/hr during the DISCOVER-AQ campaign in the summer of 2013, with values up to 140 ppbv/hr seen over the Houston shipping channel. These values are consistent with previous studies in the region (Sommariva et al., 2011). Higher concentrations of NO and larger production rates of RO_X were seen during DISCOVER-AQ than during SAFS, both of which could lead to higher $P(O_3)$."

We have also expanded slightly the comparison to the Schade and Roest study done at Floresville (Lines 597 – 603):

> "Observed isoprene at Floresville during SAFS was more than an order of magnitude larger than that reported in Schade and Roest (2016), with alkane concentrations consistent between the two studies. When the data used in Schade and Roest (2016) are subset to afternoon times and May through July, the contribution of isoprene to VOC reactivity increases to a median value of 38%, in agreement with the results presented here (Schade,

personal communication). The differences between the two studies do suggest that there could be significant seasonal and diurnal variations in OH reactivity. "

We also note that we caution against applying these results to sites beyond the SAFS monitoring sites. The satellite results do suggest that the region as a whole is NO_X-limited in the afternoon, when ozone production rates are the highest. The paper reads (lines 588 – 591):

> "While there are trees throughout the San Antonio region, the results at UTSA cannot be extrapolated to areas with far less foliage without further observations. Other VOCs could comprise a larger fraction of total OH reactivity in less vegetated areas."

Figure 7 indicates that most of the time O3 production is NOx-limited, but that there are periods, mostly in the morning, when it is VOC-limited. The text related to figure 6 (on page 16) seems to suggest that VOC limited conditions correspond to periods with low P(ROx). However this is not clear from the discussion. If this is the case, than it should be stated explicitly. On page 21 it is mentioned that the VOC limited periods in the morning correspond to high NOx (presumably rush hour emissions?) but the "flat" part of the blue curve in figure 6 is at intermediate NO levels (200-400 ppt). Are you talking about different sites? Please clarify.

We have expanded the discussion of the diurnal cycle in the ozone production regime to better illustrate this point. We have added an additional panel to figure 6 and to a new supplementary figure (Figure S3) in which, in addition to separating the data by $P(RO_X)$ values we also separate the data by VOC reactivity. Lines 377 – 416 now read:

> "Figure 6b demonstrates that the majority of observations made during SAFS were in the NO_X-limited regime. For the high $P(RO_X)$ observations, there is a steady increase in $P(O_3)$ up to the 500 pptv NO bin. Above this point, $P(O_3)$ potentially plateaus, but there were insufficient observations at higher NO to determine the location of the turnover point in ozone production. Because the majority of NO observations at UTSA were less than 500 pptv, we conclude that the site is predominantly NO_X-limited. Further observations at higher NO mixing ratios are required to determine the turnover point for ozone production in this region. The true turnover concentration for NO cannot be easily inferred by inspection of a graph of $P(O_3)$ versus [NO], however, because VOC concentrations are not constant for all points. To see if there is any variation in this relationship with VOCs, we further separate the high $P(RO_X)$ data by their VOC reactivity (Fig. SXa). VOC reactivity (VOCR) was calculated in the same manner as OH reactivity, described in section 3.3, but including only OH reactive VOC's. In addition, VOCs exclusively observed by the GC instrument were not included in the calculation as they were only available until 19 May. For data points with GC observations available, VOC reactivity increased by only 2% in the afternoon and 12% in the morning on average when including the GC observations, suggesting that this omission does not significantly affect the results. Data were then separated into low ($VOCR < 3\ s^{-1}$), medium ($3\ s^{-1} < VOCR < 6\ s^{-1}$), and high ($6\ s^{-1} < VOCR < 9\ s^{-1}$) VOC reactivity bins. For the high $P(RO_X)$ case, the relationship is similar for all VOC reactivities, showing a general increase in $P(O_3)$ with NO, further suggesting the majority of observations were NO_X-limited for high $P(RO_X)$. We note that for a constant $P(RO_X)$ value, theoretically $P(O_3)$ is expected to increase with [NO] at approximately the same rate until the turn-over point with little sensitivity to the VOC reactivity. The 5^{th} and 95^{th} percentiles of $P(RO_X)$ for the high $P(RO_X)$ are 0.42 and 0.92 pptv/s, more than a factor of two different. This

suggests that the differences in the rate of change of $P(O_3)$ with NO for the different VOC reactivities likely results from the wide range of $P(RO_X)$ values analyzed.
When looking at all points for the low $P(RO_X)$ case (Fig. 6b), there is a small peak in $P(O_3)$ at 200 pptv NO, suggesting that in a low $P(RO_X)$ environment, UTSA can be VOC-limited at higher NO mixing ratios. Separating these data points by VOC reactivity, shows more clearly the transition between the NO_X- and VOC-limited regimes. For the medium case, $P(O_3)$ first increases with [NO], peaks at 5 ppbv/hr at approximately 200 pptv [NO], and then declines to 2 ppbv/hr at 400 pptv [NO]. This peak and decline suggests that, for $P(RO_X)$ < 2 pptv/s, VOC reactivities < 6 s^{-1}, and NO > 200 pptv, the region is VOC-limited. For NO > 400 pptv, there is a slight increase in $P(O_3)$ with [NO], although the spread of data for a given [NO], also increases. For the low VOC reactivity scenario, the range of $P(O_3)$ for a given [NO] is also large compared to the mean $P(O_3)$, making it difficult to determine whether these points obey a similar relationship. As with the high $P(RO_X)$ scenario, each bin has a wide range of $P(RO_X)$ and VOC reactivities, which could lead to the large spread in data. More observations are needed to further separate the data. Separating the results by location yields the same results, although VOC reactivity at Floresville and Corpus were almost always below 3 s^{-1} due to the lower isoprene concentration at these sites in comparison to UTSA."

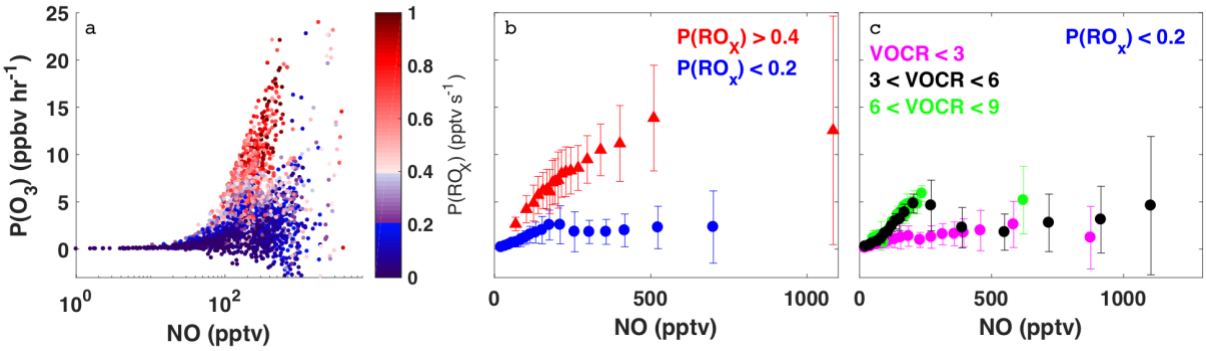

Minor Comments ————
It would be good to check the sensitivity of equation 2 to the choice of k_eff. Do the results change significantly with another value of k_eff?

We have added a paragraph in section 3.2 in which we discuss a new supplementary figure that shows the relationship between $P(O_3)$ and NO for four different values of k_{eff}. While the $P(O_3)$ value obviously changes, the overall relationship does not change, with the majority of points still being NO_X-limited. In addition, we note that the uncertainty in the k_{NO+HO2} value is greater than the uncertainty from choosing different, reasonable k_{eff} values. The paragraph (Lines 424 – 430) reads:

"Finally, the results presented here are insensitive to the value of k_{eff} chosen. Figure S4 shows the relationship between $P(O_3)$ and NO for four different values of k_{eff}: k_{NO+HO2} (the k_{eff} used in this analysis), $k_{NO+CH3O2}$, $k_{NO+IsopreneRO2}$, and assuming $k_{no+acetyl\ peroxy}$ for 10% of the value and k_{NO+HO2} for the remainder. While the magnitude of $P(O_3)$ does change with k_{eff}, the overall relationship is the same. As mentioned previously, the uncertainty in k_{NO+HO2} is larger than the uncertainty induced by the choice of k_{eff}. Additional analysis further suggests that the majority of the observations during SAFS were in the NO_X-limited regime."

Shouldn't O1D quenching by O2 be included in equation 3?

Yes, we have corrected this error.

Figure 2. Can you add the outline of San Antonio on the left panel? Is the Floresville site visible on the right panel? And can you use consistent labels? The UTSA site is labelled 1 in one panel and B in the other.

We now show the outline of the city of San Antonio in purple in the left panel. We also use numbers for all locations in both panels, using consistent numbering between the two. We have also expanded the axis limits so that we can show the Floresville SAFS site on panel b.

Figure 5. I assume that is the median of all three sites together?

That is correct. The figure caption now reads:

"…The median value for 15-minute time bins for observations at all sites is shown by the gold trace."

Characterization of Ozone Production in San Antonio, Texas Using Measurements of Total Peroxy Radicals

Daniel C. Anderson[1], Jessica Pavelec[1], Conner Daube[2], Scott C. Herndon[2], W. B. Knighton[3], Brian M. Lerner[2], J. Robert Roscioli[2], Tara I. Yacovitch[2], Ezra C. Wood[1]

[1]Department of Chemistry, Drexel University, Philadelphia, PA, USA

[2]Aerodyne Research Inc., Billerica, MA, USA

[3]Department of Chemistry and Biochemistry, Montana State University, Bozeman, MT, USA

Abstract

Observations of total peroxy radical concentrations ($[XO_2] \equiv [RO_2] + [HO_2]$) made by the Ethane CHemical AMPlifier (ECHAMP) and concomitant observations of additional trace gases made onboard the Aerodyne Mobile Laboratory (AML) during May 2017 were used to characterize ozone production at three sites in the San Antonio, Texas region. Median daytime $[O_3]$ was 48 ppbv at the site downwind of central San Antonio. Higher concentrations of NO and XO_2 at the downwind site also led to median daytime ozone production rates ($P(O_3)$) of 4.2 ppbv hr^{-1}, a factor of two higher than at the two upwind sites. The 95th percentile of $P(O_3)$ at the upwind site was 15.1 ppbv hr^{-1}, significantly lower than values observed in Houston. *In situ* observations, as well as satellite retrievals of HCHO and NO_2, suggest that the region was predominantly NO_X-limited. Only approximately 20% of observations were in the VOC-limited regime, predominantly before 11 am, when ozone production was low. Biogenic volatile organic compounds (VOC) comprised 55% of total OH reactivity at the downwind site, with alkanes and non-biogenic alkenes responsible for less than 10% of total OH reactivity in the afternoon, when ozone production was highest. To control ozone formation rates at the three study sites effectively, policy efforts should be directed at reducing NO_X emissions. Observations in the urban center of San Antonio are needed to determine whether this policy is true for the entire region.

Deleted: Observations

Deleted: s

Formatted: Not Superscript/ Subscript

Deleted: is NO_X limited for times after approximately 9:00 local time, before which ozone production is VOC-limited

1. *Introduction*

Tropospheric ozone (O_3) is a secondary air pollutant formed through a series of reactions involving volatile organic compounds (VOCs) and NO_X ($[NO_X] \equiv [NO] + [NO_2]$, where NO is nitric oxide and NO_2 is nitrogen dioxide). While tropospheric ozone exists naturally through stratospheric transport (Holton et al., 1995) and *in situ* tropospheric production, human activities have drastically perturbed these background values (Lamarque et al., 2005). Exposure to ozone adversely impacts human health, limiting lung and cardiac function, exacerbating chronic respiratory illnesses, and precipitating early mortality (Bell et al., 2006;Park et al., 2005;Jerrett et al., 2009;Silva et al., 2013). In response to these adverse impacts, in 2015 the United States Environmental Protection Agency (EPA) imposed an 8 hour ozone standard of 70 ppbv, lowering the exposure limit from the 75 ppbv standard set in 2008 (EPA, 2015). While ambient concentrations of the ozone precursor NO_X have declined significantly over much of the US (Choi and Souri, 2015;He et al., 2013;Duncan et al., 2016;Lamsal et al., 2015), reductions in ozone concentrations have been less dramatic. Background ozone concentrations have actually increased in some locations (Cooper et al., 2012;Choi and Souri, 2015); in other areas that have seen decreases in ambient ozone concentrations, such as Texas and the mid-Atlantic region, ozone still periodically exceeds the EPA standard (e.g. He et al., 2013).

Ozone production is generally classified as either NO_X- or VOC-limited (Kleinman, 1994;Thornton, 2002). Net formation of ozone occurs when NO is oxidized to NO_2 by reaction with the hydroperoxyl radical (HO_2) or an organic peroxy radical (RO_2). In the NO_X-limited regime, comparatively low concentrations of NO_X allow for the removal of RO_X radicals ($[RO_X] \equiv [OH] + [HO_2] + [RO_2]$, where OH is the hydroxyl radical) by self-reactions (e.g. Reactions R1 – R3). In the VOC-limited regime, RO_X radicals are removed from the atmosphere by reactions

Deleted: s

Deleted: termination

Deleted: radicals

with NO_X, producing less reactive compounds such as nitric acid (HNO_3) (Reactions R4 – R6). In the NO_X-limited regime, reductions in NO_X lead to reductions in O_3; while in the VOC-limited regime, reductions in NO_X without concomitant reductions in VOCs can actually increase O_3 production. One prominent example of this is the weekday/weekend effect in the Southern California Air Basin, where O_3 increases on weekends due to decreases in NO_X emissions from heavy duty diesel trucks (Pollack et al., 2012). The effective implementation of ozone reduction policies therefore requires a detailed understanding of the ozone production regime of the target area.

$$HO_2 + OH \rightarrow H_2O + O_2 \quad \text{(R1)}$$
$$HO_2 + HO_2 + M \rightarrow H_2O_2 + O_2 + M \quad \text{(R2)}$$
$$HO_2 + RO_2 \rightarrow ROOH + O_2 \quad \text{(R3)}$$
$$OH + NO_2 + M \rightarrow HNO_3 + M \quad \text{(R4)}$$
$$NO + RO_2 + M \rightarrow RONO_2 + M \quad \text{(R5)}$$
$$NO_2 + R(O)O_2 + M \rightarrow R(O)O_2NO_2 + M \quad \text{(R6)}$$

Texas is the second most populous state in the US. With multiple large urban centers and a mixture of urban and industrial emissions from petrochemical processing facilities as well as from natural gas and oil extraction, the state has complex pollution chemistry. This combination of a large population and pollution makes understanding ozone production in this region particularly important. Previous studies of ozone formation in Texas have focused primarily on Houston and the surrounding region. Mazzuca et al. (2016) used *in situ* observations of NO_X and O_3 from the DISCOVER-AQ campaign in summer 2013 along with output from the CMAQ model to find significant diurnal variability in ozone production, with higher ozone production rates ($P(O_3)$) in the morning and a transition from the VOC- to NO_X-limited regime before afternoon. Similar results were found during the TEXAQS2000, TRAMP2006, and SHARP 2009 campaigns (Mao et al., 2010;Ren et al., 2013). Multiple studies have found that anthropogenic alkenes, particularly ethylene and propylene, are major

contributors to OH reactivity and therefore O_3 production (Mao et al., 2010;Kleinman et al., 2002;Ryerson et al., 2003) in the region leading to $P(O_3)$ greater than 50 ppbv hr^{-1} (Mazzuca et al., 2016). OH reactivity is defined as the sum of the products of the concentration of species X and the reaction rate coefficient (k_{X+OH}) of X with OH (Eq. 1).

$$k_{OH} = \sum_i k_{(X+OH)}[X]_i \quad (1)$$

There have been comparatively few field campaigns, however, to study San Antonio, Texas, the seventh most populous city in the US. In July 2018, the EPA designated the San Antonio region as being in marginal non-attainment with the new 70 ppbv standard, suggesting a need to understand the O_3 formation chemistry in the region. In addition, San Antonio has a significantly different emissions profile than Houston. For example, examination of long-term VOC monitoring in Floresville, TX, a site immediately upwind of San Antonio, suggests that OH reactivity is dominated by alkanes (Schade and Roest, 2016) in contrast with the dominance of alkenes in Houston. Fig. 1 shows the trends in concentrations of ozone, NO_X, and O_X ($O_X \equiv O_3 + NO_2$) at two Texas Commission on Environmental Quality (TCEQ) monitoring sites, with one (Camp Bullis) located northwest of the urban center and the other (Pecan Valley) in the downtown area (Fig. 2b). With the lowering of the 8-hour ozone standard from 75 ppbv (dashed purple line) to 70 ppbv (solid purple line), the Camp Bullis site is much more likely to be in exceedance, while the Pecan Valley site remains below both standards. Despite noticeable decreases in maximum NO_X at both sites over the 14-year period shown here, there is little noticeable trend in ozone. This is in agreement with Choi and Souri (2015), who found a 0.07×10^{15} $cm^{-2}yr^{-1}$ decrease in tropospheric column NO_2 over San Antonio between the years 2005 and 2014 while finding an increasing trend of 0.64 ppbv yr^{-1} in the minimum value of surface

Moved (insertion) [1]
Deleted: 4
Deleted:
Formatted: Indent: First line: 0"

ozone over the same period. Further study is needed in the San Antonio region to understand the driving factors behind ozone production.

In this manuscript, we present results from the San Antonio Field Study (SAFS) conducted in the San Antonio, Texas region in May 2017. We show observations of total peroxy radical concentrations ($[XO_2] \equiv [RO_2] + [HO_2]$) from three sites in the San Antonio area, characterizing the XO_2 distribution in the region. We use these XO_2 measurements, along with observations of NO and other trace gas species, to quantify ozone production in regions up- and downwind of the urban core. Though there have been many prior determinations of $P(O_3)$ using measurements of a subset of peroxy radicals (*i.e.*, using laser-induced fluorescence measurements of HO_2 and a fraction of RO_2) (e.g. Ren et al., 2013), this is one of the few determinations of ozone production using the direct observation of total peroxy radicals (Sommariva et al., 2011). Combined with quantification of the primary production of RO_X radicals ($P(RO_X)$) and satellite retrievals of HCHO and NO_2, we determine the ozone production regime in San Antonio. Finally, we explore the main contributors to OH reactivity in the region.

2. Methodology

2.1 Campaign Description

The SAFS campaign was conducted from 11 to 31 May 2017 at several sites in the greater San Antonio region. We describe measurements made on the Aerodyne Mobile Laboratory (AML) at three sites: the University of Texas San Antonio (UTSA) from 11 to 16 May and from 27 to 31 May, Floresville, Texas from 16 to 21 May, and Lake Corpus Christi (Corpus) from 21 to 26 May. The sites were chosen to determine the impact of various emission sources on ozone formation affecting San Antonio. During May in southeastern Texas, the prevailing wind direction is southeasterly, coming off the Gulf of Mexico. UTSA is located

Deleted: s

Deleted: ($XO_2 \equiv RO_2 + HO_2$)

northwest (*i.e.* downwind) of downtown San Antonio (Fig. 2a) while the Floresville and Corpus sites were both located upwind of the city. This allows for the determination of background values of compounds through observation at the Floresville and Corpus sites, while observations at UTSA are more representative of air photochemically processed with urban emissions. We define background here as values upwind of the UTSA site. The AML was situated at all sites to minimize influence from local emissions. At UTSA, the AML was located in a mostly vacant parking lot about 1 km south of the nearest major roadway. In Floresville and Corpus, there were no nearby major roadways, local traffic was at a minimum, and influence from local point and mobile sources was limited. Potential influences from transient local sources (e.g. lawn mowers and jet skis) were removed in the same manner as interference from the generator emissions described below.

The AML is outfitted to measure a suite of gas- and particle-phase atmospheric species (Herndon et al., 2005). All instrument inlets were mounted approximately 15 m above ground level on a retractable tower located near the AML. At both the Floresville and UTSA sites, the AML was powered through connection to the local electric utility while at Corpus a diesel generator was used. Although the generator was situated downwind of the instrument inlets, some stagnation and recirculation did occur, allowing for occasional sampling of generator exhaust. Air parcels affected by the generator exhaust were removed through analysis of CO observations. A filter for generator-influenced air was created by determining the minimum CO value over a 100 s period every 5 minutes. Any air parcel with a CO mixing ratio 10 ppbv higher than this minimum was assumed to be impacted by a local transient source, including the generator.

Trace gases measured during SAFS and used in this study are summarized here. Unless otherwise indicated, data used in this study were reported as 1-minute averages and then averaged to the 2-minute Ethane CHemical AMPlifier (ECHAMP) time base, described in the following section. NO_2 was measured at 1 Hz via Cavity Attenuated Phase Shift (CAPS) spectroscopy (Kebabian et al., 2005;Kebabian et al., 2008). Nitric oxide (NO) was measured at 0.1 Hz through the same inlet as NO_2 and O_3 using a Thermo Fisher 42i-TL chemiluminescence analyzer, while O_3 was measured with a 2B-Tech model 205 ultraviolet (UV) absorption instrument. Uncertainties (2σ) of the NO, NO_2, and O_3 observations on the ECHAMP measurement time scale are below 5%. The above instruments were zeroed every 15 minutes with humidity-matched zero air. The zero air was generated by passing ambient air through an Aadco ZA30 Catalyst system for VOC removal and through Purafill Chemisorbant Media, a potassium permanganate based scrubber, for NOx removal.

Quantum Cascade – Tunable Infrared Laser Direct Absorption Spectrometers (QC-TILDAS) from Aerodyne Research Inc. (ARI) were used to measure CO and H_2O (2200 cm^{-1}; measurement wave number), HCHO (1765 cm^{-1}), CH_4 and C_2H_6 (2990 cm^{-1}), H_2O_2 (1277 cm^{-1}), and C_3H_8 (2965 cm^{-1}) (McManus et al., 2015). A Proton Transfer Reaction – High Resolution – Time of Flight (PTR-HR-ToF) mass spectrometer was used to measure isoprene, acetaldehyde, acetone, benzene, methanol, the sum of monoterpenes, the sum of methyl vinyl ketone (MVK) and methacrolein, and toluene. Typical measurement uncertainties were on the order of 25%. Finally, a prototype of a commercially-available gas chromatograph from ARI with electron-impact time-of-flight mass spectrometer (GC-EI-ToF-MS) was used to measure a suite of VOCs, including isoprene, 1,2,3-trimethylbenzene, ethyl benzene, cyclohexane, *n*-heptane, *n*-hexane, *n*-octane, *n*-pentane, *o*-xylene, and the sum of *m*- and *p*- xylenes. The GC

Deleted: Differential

Deleted: instrument

Deleted:

sampled with a multi-component adsorbent trap (Pollmann et al., 2006) for a 5 minute integration period every 20 minutes. GC observations are unavailable for 20-30 May. While toluene and *m*- and *p*- xylene measurement uncertainty was on the order of 20%, typical measurement uncertainties of other observed species, except isoprene, were on the order of 10%.

While there were two independent observations of isoprene, there were limitations with both methods. It was determined that the actual isoprene concentration in the calibration standard used in the field for the PTR had degraded over time, resulting in erroneously high isoprene values. On the other hand, the GC was not calibrated for isoprene during the campaign and observations are only available for half the time. As a result, we use the PTR isoprene from the entire campaign scaled to the GC values, using a GC isoprene sensitivity determined after the campaign. This method results in an estimated isoprene uncertainty of ≈30% (1σ). See the SI for more information.

Temperature, wind speed, and wind direction were measured at the top of the inlet tower with a 3D RMYoung (Model 81000RE) sonic anemometer. Atmospheric pressure observations used in this study were taken from the National Weather Service observations at the San Antonio International Airport for the UTSA and Floresville sites and from the Corpus Christi International Airport for the Corpus site. NO_2 photolysis frequencies (J_{NO2}) were measured via a filter radiometer (MetCon, GmbH) located on top of the AML (Shetter et al., 2003;Stark et al., 2007).

2.2 ECHAMP

Total peroxy radical concentrations ($[XO_2]$) were measured via chemical amplification by the ECHAMP instrument. A complete instrument description can be found in Wood et al. (2017), and only the most relevant details are summarized here, including a new sampling

Deleted: ing

Deleted: Supplementary Information (

Deleted:)

Deleted: s

system that includes an integrated, remotely-controlled RO_X calibration source. Briefly, ECHAMP measures total XO_2 concentration at a two-minute resolution by reacting peroxy radicals with excess NO and ethane (C_2H_6). Through a series of chain reactions, each XO_2 radical produces approximately 20 NO_2 molecules (depending on the relative humidity (RH)), which are then measured with a commercially available NO_2 monitor. Because this NO_2 monitor also measures ambient O_3 and NO_2 (O_X), a second channel and dedicated NO_2 monitor are used to only measure the sum of [O_3] and [NO_2]. The difference between the two channels, divided by the "amplification factor" of ~20, yields the XO_2 concentration.

The inlet box is a 39 cm × 44 cm × 16 cm fiberglass, rainproof electrical enclosure. The box was mounted at the top of the sampling tower and connected to the rest of the instrument via a bundle of tubes and electrical cables. Ambient air was sampled at a flow rate of 6.5 LPM through 76 mm of 3.6 mm inner diameter (ID) glass into the inlet box (see Fig. S1 for a schematic of the plumbing). The glass was internally coated with halocarbon wax to minimize wall losses of XO_2. The flow was sub-sampled into two, 1.9 cm^3 reaction chambers at a flow rate of 1.1 LPM each. Temperature and RH of the remaining 4.5 LPM of sampled air were measured with a Vaisala probe (Model HMP60). Laboratory tests over a range of flow rates and RH have demonstrated sampling losses of HO_2 of less than 3% and negligible losses of CH_3O_2 (Kundu et al., 2019).

Reaction chambers cycled every minute between an amplification mode and a background mode, for a total cycle time of 2 minutes. In both modes, 25 sccm of 39.3 ppmv NO in N_2 (Praxair) was added at the beginning of the reaction chamber, resulting in a final NO mixing ratio of 0.90 ppmv. In amplification mode, 35 sccm of a 42.2% ethane mixture in N_2 (Praxair) was also added to the sampled air at the beginning of the reaction chamber. The radical

Formatted: Indent: First line: 0.5"

Deleted: relative humidity (

Deleted:)

Deleted: [Kundu *et al*., in preparation]

propagation scheme shown in reactions R7 – R13, in which Reactions (R9) – (R13) repeat numerous times, results in formation of NO_2. The number of NO_2 molecules formed per XO_2 molecule sampled is known as the amplification factor (F) and varies with RH. During SAFS, F was 23 for dry air and decreased to 12 at 58% RH. The two calibration methods used to determine F are described below and more fully in the SI. At 15.2 cm downstream of the NO/C_2H_6 injection point, 35 sccm of N_2 was added to the flow. In the background chamber, the N_2 and C_2H_6 flows were switched (N_2 was added upstream, and C_2H_6 was added downstream), allowing XO_2 radicals to react with NO to form HONO or alkyl nitrates before 35 sccm of the 42.2% ethane mixture was added at the end of the reaction chamber. The resultant NO_2 from each chamber was then measured with separate, dedicated CAPS instruments. Total XO_2 was then determined by the difference between the two NO_2 measurements divided by F.

$$RO_2 + NO \rightarrow RO + NO_2 \quad (R7)$$
$$RO \rightarrow HO_2 + \text{products} \quad (R8)$$
$$HO_2 + NO \rightarrow OH + NO_2 \quad (R9)$$
$$OH + C_2H_6 \rightarrow H_2O + C_2H_5 \quad (R10)$$
$$C_2H_5 + O_2 + M \rightarrow C_2H_5O_2 + M \quad (R11)$$
$$C_2H_5O_2 + NO \rightarrow C_2H_5O + NO_2 \quad (R12)$$
$$C_2H_5O + O_2 \rightarrow CH_3CHO + HO_2 \quad (R13)$$

The CAPS instruments were calibrated for NO_2 before, after, and once during deployment via quantitative reaction of known concentrations of O_3 generated with a 2B Technologies ozone generator (Model 306) with excess NO. This ozone source agreed within 1% with a separate Thermo ozone generation source (Model 49C). All NO_2 calibrations agreed within 5%. The amplification factor (F) was determined by producing known amounts of peroxy radicals by two calibration methods: photolysis of H_2O and of CH_3I. Both methods are described in more detail in the SI. Briefly, the H_2O photolysis method is similar to that used by most HO_X instruments, in which H_2O was photolyzed at a wavelength of 184.9 nm to form an equimolar

Formatted: Font:12 pt
Formatted: Left
Formatted Table
Formatted: Font:12 pt
Formatted: Left
Formatted: Font:12 pt
Formatted: Left
Formatted: Left
Formatted: Font:12 pt
Formatted: Left
Formatted: Font:12 pt
Formatted: Font:12 pt
Formatted: Left
Formatted: Font:12 pt
Formatted: Left

mixture of OH and HO_2 (Mihele and Hastie, 2000;Faloona et al., 2004). This mixture was then reacted with H_2 to convert the OH into HO_2. Radical concentrations were quantified using the relevant spectroscopic parameters and the measured H_2O and O_3 concentrations in the calibration gas.

The second calibration method was based on 254 nm photolysis of CH_3I in humidified air, producing the CH_3O_2 radical. The radical concentration is quantified by reaction of the CH_3O_2 with NO in the absence of C_2H_6, producing 1.86 NO_2 molecules per CH_3O_2. The H_2O photolysis method was performed 6 times, while the CH_3I method was performed once during the field campaign, on 31 May. Both methods were repeated twice in the laboratory after the campaign. Observations from ECHAMP agreed within 12% with the H_2O photolysis calibration source operated by Indiana University during a comparison study in 2015 (Kundu et al., 2019). For the XO_2 observations described in this paper, we use the CH_3I calibration. While both methods agree within uncertainty, the H_2O photolysis method was only conducted for RH values of less than approximately 20%, much lower than typical ambient RH. See the SI for further information.

Deleted: [Kundu et al., in preparation]

The total 2σ accuracy for XO_2 during SAFS was approximately 25%. Calibrations were not performed at RH values greater than 71%. Therefore, we omit all observations with a sample RH greater than 71%. Approximately 85% of these high RH points were observed at nighttime, so we only consider daytime data (7:00 – 20:00 local time) unless otherwise indicated.

2.3 Calculation of $P(O_3)$ and $P(RO_X)$

We use measurements of XO_2 and NO to calculate the gross rate of ozone production $P(O_3)$ using Eq. (2), in which k_{NO+HO2} is the reaction constant for the reaction of NO with HO_2 and k_i is the reaction constant for NO with an organic peroxy radical $[RO_2]_i$. We note that this is

Deleted: 1

more accurately described as the rate of odd oxygen (O_X) production. Because ECHAMP only measures the sum of peroxy radicals and not their speciation, we assume a simplified form of this relationship (Eq. 3), where k_{eff} is an effective rate constant taken as that of k_{NO+HO2}. Box modeling results for this site, which will be discussed more fully in a forthcoming paper, show the dominant XO_2 species are HO_2, CH_3O_2, and isoprene RO_2. At 298 K, k_{NO+HO2} is within 10% of the k values for the reaction of NO with CH_3O_2 and isoprene RO_2 (Orlando and Tyndall, 2012), supporting our choice of k_{eff}. Further, while the reaction of NO with acetyl peroxy radicals is approximately 2.5 times faster than with other peroxy radicals at 298K, box modeling results suggest that these radicals comprise only 5 – 10% of total XO_2, resulting in an average difference in $P(O_3)$ of 15% from the k_{NO+HO2} value used here. This uncertainty is comparable to the total uncertainty of the k_{NO+HO2} rate constant, estimated as 15% (Sanders et al., 2011). As will be shown in Section 3.2, our conclusions are insensitive to the value of k_{eff} chosen. Uncertainty in gross $P(O_3)$ results from uncertainty in the NO and XO_2 measurements, 5% and 25%, respectively, and k_{eff}, whose uncertainty we estimate at 23%, determined by adding the uncertainty in the k_{NO+HO2} rate constant and the uncertainty in the choice of k_{eff} in quadrature. This results in a total $P(O_3)$ uncertainty of 34%.

$$P(O_3)_{Gross} = k_{NO+HO2}[NO][HO_2] + [NO]\sum_i k_i[RO_2]_i \quad (2)$$

$$P(O_3)_{Gross} = k_{eff}[NO][XO_2] \quad (3)$$

$$L(O_3) = \left(\frac{k_{O1D+H2O}[H_2O]}{k_{O1D+H2O}[H_2O] + k_{O1D+N2}[N_2] + k_{O1D+O2}[O_2]} J_{O1D} + k_{OH+O3}[OH] + k_{HO2+O3}[HO_2] + \sum_i k_{alkene-i}[alkene_i]\right)[O_3] + k_{OH+NO2}[OH][NO_2][M] \quad (4)$$

The net formation rate of O_3 is equal to $P(O_3)_{Gross} - L(O_3)$. In order to tie $P(O_3)$ completely to observations, we report only gross $P(O_3)$, not net $P(O_3)$. That is, we only calculate

Deleted: 2
Deleted: 2
Deleted:
Deleted: (Atkinson et al., 2004)
Deleted: 5
Deleted: 6
Deleted: $Prod.$)
Deleted:)
Deleted: 1
Formatted Table
Deleted: 2
Deleted: $Prod$
Deleted:)
Deleted: $P(O_3)_{Loss}$
Deleted: $k_{alkenes+O3}[alkenes]$

the production term (Eq. 2) and not the loss term (Eq. 4) for net ozone production. Calculation of the loss term requires knowledge of the concentration of OH and alkenes as well as the fraction of total XO_2 comprised of HO_2, none of which were measured during SAFS. Alkene concentrations, except for isoprene and monoterpenes, were not measured during SAFS. Estimating the alkene loss term using concentrations from nearby TCEQ monitoring sites, suggests that O_3 loss due to this pathway is negligible for the data analyzed here, and we omit this from our calculation of ozone loss. To estimate OH and the fraction of XO_2 comprised of HO_2 and to determine whether analyzing only gross $P(O_3)$ affects our conclusions, we used the Framework for 0-Dimensional Atmospheric Modeling (F0AM) box model (Wolfe et al., 2016b) to calculate OH and the fraction of RO_2 comprised of HO_2. A description of the model setup can be found in the SI. For data points that were not modeled due to missing model constraints, these values were estimated from interpolation of modeled values, if observations were made within two hours of a modeled data point, or from site-specific mean daily profiles if no modeled points were available. Using these modeled-derived values for OH and the HO_2 fraction, median $L(O_3)$ for daytime observations at all sites were determined to be 0.90 ppbv/hr, which is 16% of the gross production rate.

We use Eq. (5) to calculate the primary RO_X production rate. Here, $P(RO_X)$ is the RO_X production rate, J indicates photolysis rate, and $k_{O1D+H2O}$, k_{O1D+O2}, and k_{O1D+N2} are the reaction rate constants for the reaction of O_{1D} with the indicated species. The Tropospheric Ultraviolet and Visible (TUV) model was used to calculate photolysis rate constants (J values), which were then scaled to the measured J_{NO2}. HONO was not measured during SAFS. We estimate HONO concentrations assuming an upper limit to the $[HONO]/[NO_X]$ ratio of 0.04 as described in Lee et al. (2013). This is an upper bound on the HONO concentration and thus on HONO contribution

Deleted: concentration and t

Deleted: neither

Deleted: observed

Deleted: AQRP

Deleted: these values

Deleted: and

Deleted: results

Deleted: average

Deleted: chemical ozone loss rates

Deleted: 5

Deleted: and

Deleted: the loss rate was, on average,

Deleted: 0

Deleted: This is well within the overall uncertainty of the calculated gross production rate. As a result, we report only gross production.

Deleted: Similarly,

Deleted: w

Deleted: use the expression shown in

Deleted: 43

Deleted: H_2O and air

Deleted: , and M is the concentration of $O_2 + N_2$

to $P(RO_X)$. Alkene concentrations were estimated from nearby TCEQ monitoring sites, as described in Sect. 3.3. Alkene ozonolysis was calculated to have a negligible impact on $P(RO_X)$ and is omitted from the analysis.

$$P(RO_X) = 2J_{O1D}[O_3]\frac{k_{O1D+H2O}[H_2O]}{k_{O1D+H2O}[H_2O]+k_{O1D+N2}[N_2]+k_{O1D+O2}[O_2]} + 2J_{HCHO}[HCHO] + 2J_{CH3CHO}[CH_3CHO] + 2J_{Acetone}[CH_3COCH_3] + 2J_{H2O2}[H_2O_2] + J_{HONO}[HONO] \quad (5)$$

Total $P(RO_X)$ peaks at midday at about 0.65 pptv s^{-1} on average and is dominated by the ozone and HCHO terms, terms 1 and 2 from Eq. (5), respectively, with contributions from the other observed species totaling less than 5% on average. Contributions from HONO were generally less than 0.1 pptv s^{-1}, even assuming the upper bound in the HONO to NO_X ratio used here.

2.4 Satellite Data

We use observations of NO_2 and HCHO from the Ozone Monitoring Instrument (OMI) to provide a remotely-sensed estimate of the surface ozone production regime in San Antonio (Duncan et al., 2010;Ring et al., 2018). OMI has a local overpass time of about 13:30 and provides daily, global coverage. The instrument measures backscattered solar radiation in the UV/visible region, allowing for differential optical absorption spectroscopy (DOAS) type retrievals of multiple species, including NO_2 and HCHO.

For NO_2, we use the NASA Goddard Space Flight Center (GSFC) version 3 level 2 tropospheric column product (Bucsela et al., 2013;Krotkov et al., 2017) gridded to 0.25º latitude × 0.25º longitude resolution. For HCHO, we use the version 3 level 2 reference sector corrected swath product from the Harvard-Smithsonian Astrophysical Observatory (SAO) retrieval (González Abad et al., 2015) also on a 0.25º latitude × 0.25º longitude grid. For both OMI products, we use only pixels that satisfy quality and row anomaly flags, have a cloud fraction less than 30%, and a solar zenith angle less than 70º. Additionally, data from the two outer most

Deleted: Alkenes, with the exception of the biogenic species isoprene and the sum of monoterpenes, were not measured by the AML during SAFS.

Deleted: $[M]$

Deleted: 43

Deleted: 43

pixels are removed due to their large footprint (28km × 150km) compared to the nadir view.

We analyze the HCHO to NO_2 ratio using OMI data from May to July 2017. While SAFS lasted only one month, missing data due to cloud cover, the row anomaly, and other factors necessitate a longer time period for data averaging. To calculate the ratio of HCHO to NO_2, we first calculate the standard deviations (σ) of the HCHO and NO_2 data at each grid point. When calculating the ratio, we only include days within 2σ of the average HCHO and NO_2 observations and only include grid boxes that have at least 10 days with coincident observations of both species.

3. Results

3.1 Distribution of Ozone and its precursors

The highest ozone mixing ratios observed at UTSA were on 14 and 15 May, reaching a maximum near 80 ppbv, while daytime values typically varied between 40 and 60 ppbv during the remainder of the campaign (Fig. 3). Median daytime [O_3] at all three measurement sites was 37 ppbv (Fig. 4a). Median ozone was 18 ppbv higher at UTSA than at the background site in Floresville. Although the highest ozone values were seen at UTSA, there was significant overlap in the ozone distribution between the UTSA and Corpus sites. Consistent with the higher O_3 abundance, concentrations of the O_3 precursors isoprene, NO, and XO_2 were also highest at the UTSA site. Median isoprene concentrations, one of the largest contributors to OH reactivity as will be shown later, was almost two orders of magnitude larger at UTSA (1.2 ppbv) than at the other sites (0.05 and 0.03 ppbv at Floresville and Corpus, respectively). While the difference in median [NO] at the sites was not as extreme, a much larger range was seen at UTSA, where the 95^{th} percentile of observations was above 2 ppbv. Similar results are seen for the [XO_2] distribution (Fig. 4c), with the highest XO_2 mixing ratios (90 pptv) coinciding with the maximum

O_3. Median [XO_2] was approximately 1.5 times higher at the UTSA site (37 pptv) than at Floresville (26 pptv) and Corpus (25 pptv).

XO_2 concentrations showed a distinct diurnal profile (Fig. 5). Overnight values were approximately constant with a median of around 10 pptv, until a small decline after 3:00. A steady increase in [XO_2] began at 9:00, with a peak of 50 pptv at 15:00 and then a decline to the overnight value by 20:00. The shape of this profile is in agreement with other observations of peroxy radicals from a variety of chemical environments (Sanchez et al., 2016;Mao et al., 2010;Whalley et al., 2018). Noise in the nighttime data is a result of higher RH and thus degraded precision of the ECHAMP measurement technique and is not an indication of significant nighttime variability. Even though we have filtered for data points with RH greater than 71% as discussed in Sect. 2.2, nighttime RH is higher than daytime values, on average, decreasing measurement precision. Daytime variability resulted from changes in insolation and biogenic VOC concentrations. The days that showed little or no diurnal profile at UTSA and Corpus were overcast, as evidenced by low J_{NO2} (Fig. 3). Concentrations of isoprene and the sum of methyl vinyl ketone (MVK) and methacrolein, both isoprene degradation products, were at a maximum when [XO_2] peaked at 90 pptv.

The higher O_3 concentrations at UTSA are consistent with its location downwind of the urban core of San Antonio. Figure S2 shows wind roses colored by ozone and the ozone precursors described above. The wind direction while at UTSA was predominantly southeasterly, in agreement with the climatological average for the region. The highest ozone mixing ratios, as well as the highest XO_2 and isoprene, were seen when air parcels originated from this direction, travelling over the city. The highest [NO] (greater than 2.2 ppbv), however, was seen with northerly and northeasterly winds. This is likely because of the proximity of a

Deleted: a 1

major highway north of the UTSA site, which would provide a source of recently-emitted, less processed emissions than in air parcels that travelled from downtown San Antonio. The CO distribution by wind direction (not shown) is consistent with this explanation.

3.2 Ozone production

The highest $P(O_3)$ values (and highest [NO] and $[XO_2]$) were observed at UTSA. Median $P(O_3)$ between 7:00 and 20:00 at UTSA was 4.1 ppbv hr^{-1}, compared to just over 1 ppbv hr^{-1} at both Floresville and Corpus. The 95th percentile, 12.6 ppbv hr^{-1}, is significantly lower than rates found in Houston, which frequently topped 40 ppbv hr^{-1} (Mazzuca et al., 2016;Mao et al., 2010). As with $[O_3]$ and $[XO_2]$, the highest $P(O_3)$ rates occurred when winds travelled over downtown San Antonio.

Figure 6a shows the variation in $P(O_3)$ with [NO], where the data points have been colored by $P(RO_X)$ for all observations taken during SAFS. The relationship for the subset of observations exclusively at UTSA is essentially identical. In general, $P(O_3)$ increases with [NO], although a wide range of $P(O_3)$ exists for a given value of NO. For a constant value of [NO], $P(O_3)$ is consistently higher at higher $P(RO_X)$. Figure 6b shows the same data as panel 6a but binned both by NO mixing ratio and $P(RO_X)$. All $P(O_3)$ observations have been separated into NO bins with an equal number of observations, as well as into two bins of $P(RO_X)<0.2$ and $P(RO_X)>0.4$. The values of $P(RO_X)$ were chosen to represent the low and high ranges of $P(RO_X)$ observed during SAFS. The conclusions drawn from the results are insensitive to the values chosen for these bins.

Figure 6b demonstrates that the majority of observations made during SAFS were in the NO_X-limited regime. For the high $P(RO_X)$ observations, there is a steady increase in $P(O_3)$ up to the 500 pptv NO bin. Above this point, $P(O_3)$ potentially plateaus, but there were insufficient observations at higher NO to determine the location of the turnover point in ozone production.

Deleted: fresher

Deleted: Figure 6

Formatted: Font:(Default) Times New Roman

Formatted: Font:(Default) Times New Roman

Deleted: Figure 6

Deleted: 15

Deleted: 5

Formatted: Font:(Default) Times New Roman

Deleted: Figure 6

Because the majority of NO observations at UTSA were less than 500 pptv, we conclude that the site is predominantly NO_X-limited. Further observations at higher NO mixing ratios are required to determine the turnover point for ozone production in this region. The true turnover concentration for NO cannot be easily inferred by inspection of a graph of $P(O_3)$ versus [NO], however, because VOC concentrations are not constant for all points. To see if there is any variation in this relationship with VOCs, we further separate the high $P(RO_X)$ data by their VOC reactivity (Fig. S3). VOC reactivity (VOCR) was calculated in the same manner as OH reactivity, described in section 3.3, but including only OH reactive VOCs. In addition, VOCs exclusively observed by the GC instrument were not included in the calculation as they were only available until 19 May. For data points with GC observations available, VOC reactivity increased by only 2% in the afternoon and 12% in the morning on average when including the GC observations, suggesting that this omission does not significantly affect the results. Data were then separated into low (VOCR < 3 s^{-1}), medium (3 s^{-1} < VOCR < 6 s^{-1}), and high (6 s^{-1} < VOCR < 9 s^{-1}) VOC reactivity bins. For the high $P(RO_X)$ case, the relationship is similar for all VOC reactivities, showing a general increase in $P(O_3)$ with NO, further suggesting the majority of observations were NO_X-limited for high $P(RO_X)$. We note that for a constant $P(RO_X)$ value, theoretically $P(O_3)$ is expected to increase with [NO] at approximately the same rate until the turn-over point with little sensitivity to the VOC reactivity. The 5th and 95th percentiles of $P(RO_X)$ for the high $P(RO_X)$ are 0.42 and 0.92 pptv s^{-1}, more than a factor of two different. This suggests that the differences in the rate of change of $P(O_3)$ with NO for the different VOC reactivities likely results from the wide range of $P(RO_X)$ values analyzed.

When looking at all points for the low $P(RO_X)$ case (Fig. 6b), there is a small peak in $P(O_3)$ at 200 pptv NO, suggesting that in a low $P(RO_X)$ environment, UTSA can be VOC-limited

Moved (insertion) [4]
Deleted: 7a
Deleted: Xa
Deleted:
Moved (insertion) [5]
Deleted: should
Deleted: regardless of
Deleted:
Formatted: Superscript
Formatted: Superscript
Formatted: Indent: First line: 0.5"
Deleted: F

at higher NO mixing ratios. Separating these data points by VOC reactivity, shows more clearly the transition between the NO_X- and VOC-limited regimes. For the medium case, $P(O_3)$ first increases with [NO], peaks at 5 ppbv hr^{-1} at approximately 200 pptv [NO], and then declines to 2 ppbv hr^{-1} at 400 pptv [NO]. This peak and decline suggests that, for $P(RO_X) < 0.2$ pptv/s, VOC reactivities < 6 s^{-1}, and NO > 200 pptv, the region is VOC-limited. For NO > 400 pptv, there is a slight increase in $P(O_3)$ with [NO], although the spread of data for a given [NO], also increases. For the low VOC reactivity scenario, the range of $P(O_3)$ for a given [NO] is also large compared to the mean $P(O_3)$, making it difficult to determine whether these points obey a similar relationship. As with the high $P(RO_X)$ scenario, each bin has a wide range of $P(RO_X)$ and VOC reactivities, which could lead to the large spread in data, suggesting the need for further observations. Separating the results by location yields the same results, although VOC reactivity at Floresville and Corpus were almost always below 3 s^{-1} due to the lower isoprene concentration at these sites in comparison to UTSA.

Ozone production rates in VOC-limited regime are typically below 5 ppbv hr^{-1} and constitute only 20% of the observations examined here, suggesting that the all three SAFS sites are predominantly NO_X-limited. The majority of the VOC-limited points here (75%) occur before 11 EDT, when NO concentrations are higher and isoprene emissions and VOC reactivity are low. This is in agreement with the L_n/Q diurnal profile discussed below. For the NO_X-limited points, increases in VOC concentrations are expected to have a small impact on $P(O_3)$; for the VOC-limited points, increases in VOCs will lead to increased $P(O_3)$.

Finally, the results presented here are insensitive to the value of k_{eff} chosen. Figure S4 shows the relationship between $P(O_3)$ and NO for four different values of k_{eff}: k_{NO+HO2} (the k_{eff} used in this analysis), $k_{NO+CH3O2}$, $k_{NO+IsopreneRO2}$, and assuming $k_{no+acyl\ peroxy}$ for 10% of the value

Deleted:

Deleted: lowest two VOC reactivity bins (VOCR < 3 s^{-1} and 3 s^{-1} < VOCR < 6 s^{-1}),low and

Deleted: s

Deleted: , and then a slowly increases at higher [NO]. This shape is significantly more pronounced for the 3 s^{-1} < VOCR < 6 s^{-1}medium VOC reactivity case, with $P(O_3)$ peaking at 5 ppbv/hr at 200 pptv of NO and then dropping

Deleted: these

Moved up [5]: We note that for a constant $P(RO_X)$ value, theoretically $P(O_3)$ should increase with NO at approximately the same rate until the turn-over point regardless of VOC reactivity.

Deleted: While the medium and high cases generally follow the same shape, the low VOC reactivity case shows a averaging over a range of $P(RO_x)$ or a missing $P(RO_X)$ source. Further observations are needed to determine the cause.

Deleted: Because $P(O_3)$ is typically only 1 ppbv hr^{-1} when $P(RO_X)$ is at these levels, however, ozone production in this regime is negligible

Deleted: this

Deleted: .

Deleted: X

and k_{NO+HO2} for the remainder. While the magnitude of $P(O_3)$ does change with k_{eff}, the overall relationship is the same. As mentioned previously, the uncertainty in k_{NO+HO2} is larger than the uncertainty induced by the choice of k_{eff}. Additional analysis further suggests that the majority of the observations during SAFS were in the NO_X-limited regime.

These results are consistent with the diurnal profile of the ozone production regime as determined by the separate "L_N/Q" metric, which is the ratio of the RO_X loss rate due to reactions with NO_X (e.g., R3) to the total RO_X loss rate (Q) (Kleinman, 2005). In general, when more than half of the RO_X loss is due to reaction with NO_X species ($L_N/Q > 0.5$) then $P(O_3)$ is VOC-limited, whereas when the majority of RO_X loss is due to peroxy radical self-reactions ($L_N/Q < 0.5$) $P(O_3)$ is NO_X-limited. The Framework for 0-Dimensional Atmospheric Modeling (F0AM) photochemical box model (Wolfe et al., 2016b), constrained to observations, was used to model the parameters needed to calculate L_N/Q at the SAFS sites. A full description of the model setup is in the SI. Using the box model results and the method described in Kleinman (2005), we calculated L_N/Q for all box-modeled observations at UTSA (Fig. 7). A clear diurnal pattern is evident with an early morning maximum and then a quick decline to $L_N/Q < 0.5$ at 9:00, after which the ratio remains below 0.1 for the remainder of the day. At 18:00, however, the ratio does begin to increase, though remaining well in the NO_X-limited space. While L_N/Q is highest in the morning, $P(O_3)$ is at a minimum during this time period, suggesting that there is little O_3 production when $P(O_3)$ is VOC-limited. Furthermore, time periods where ozone was found under VOC-limited conditions were likely confined to a relatively small volume of air in the shallow, morning boundary layer. This transition from VOC- to NO_X-limited between morning and afternoon is consistent with other locations (Mazzuca et al., 2016;Mao et al., 2010;Ren et al.,

Moved up [4]: The true turnover concentration for NO cannot be easily inferred by inspection of a graph of $P(O_3)$ versus [NO], however, because VOC concentrations are not constant for all points.

Deleted: does

Deleted: .

2013) and the high NO concentrations that build up in the morning from local traffic and a low boundary layer.

Finally, remotely sensed observations of NO_2 and HCHO from the OMI satellite corroborate the conclusion that ozone production in San Antonio is NO_X-limited. The ratio of column HCHO to tropospheric column NO_2 has been used as an indicator of the ozone production regime in multiple regions (Duncan et al., 2010;Ring et al., 2018). According to Duncan et al. (2010), a region is considered NO_X-limited when this ratio is greater than 2, VOC-limited for values less than 1, and in a transition region for ratios between 1 and 2. Other studies dispute these ranges, claiming that, in Houston, the NO_X-limited regime only begins for a ratio greater than 5 (Schroeder et al., 2017). Figure 2 shows the ratio averaged over the months May – July 2017 over Texas. In agreement with the *in situ* observations and the above analysis, the satellite data places all three locations in the NO_X-limited regime with ratios much greater than 5. Though they provide much higher spatial coverage, polar orbiting satellite observations are limited in that they provide coverage once daily and that data must be averaged over a long period to gain meaningful statistics. Likewise, because of the satellite footprint, any small regions in urban centers that may be VOC-limited might not be evident here because of spatial averaging. Nevertheless, the combination of satellite and *in situ* observations clearly demonstrates that, at least at the three measurement sites, ozone production was NO_X-limited.

3.3 OH Reactivity

In contrast with Houston, the OH reactivity, and thus ozone production, at the UTSA measurement site was driven by biogenic species, particularly isoprene. Figure 8 shows the OH reactivity for the UTSA and Floresville sites. Observations after 19 May were excluded because of the lack of GC observations. Concentrations of all observed OH reactive species were used to calculate the total OH reactivity. These values were then divided into 5 groups: biogenics

Deleted: Figure 2

Formatted: Font:(Default) Times New Roman

Deleted: Figure 8

Formatted: Font:(Default) Times New Roman

Deleted: OH reactivity is defined as the sum of the products of the reaction rate coefficient of a species with the concentration of that species (Eq. 4).

(isoprene, MVK, methacrolein, and α-pinene), carbonyls (HCHO and acetaldehyde), alkanes (ethane, propane, cyclohexane, octane, heptane, hexane, and pentane), NO_X, CO, CH_4, O_3, and other (benzene, 1,2,4-trimethylbenzene, ethyl benzene, toluene, *o*-, *p*-, and *m*-xylene, methanol, and C_2H_2).

OH reactivity varied substantially at the two sites in both magnitude and relative importance of the individual constituents. Overall, average afternoon OH reactivity at UTSA and Floresville were 12 and 4.0 s^{-1}, respectively. While the main contributors to OH reactivity varied between morning and afternoon at both sites, the total reactivity did not show significant variation. The higher OH reactivity at UTSA is consistent with the higher $P(O_3)$ rate and XO_2 concentrations. At UTSA, the predominant contributors to OH reactivity were NO_X in the morning and biogenic VOCs in the afternoon, comprising 46% and 55% of OH reactivity, respectively. Isoprene dominated the biogenic contribution, with less than 10% of total OH reactivity resulting from monoterpenes, which have been assumed to be 100% α-pinene. Although the contribution of biogenic VOCs was lower at Floresville than at UTSA, they were still the largest component of OH reactivity in the afternoon. The significant contribution to OH reactivity from NO_X during the morning is consistent with large on-road emissions and a low boundary layer as well as with the VOC-limited nature of O_3 production in the morning. During these morning hours, when the region is VOC-limited and $P(RO_X)$ is generally less than 0.2 pptv/s, NO can frequently exceed 500 pptv (Fig. 6c), as compared to the campaign median of 225 pptv. CO and carbonyls were the other major contributors to OH reactivity at all locations, with CO being the dominant contributor at Floresville in the morning. Because one of the dominant contributors to HCHO production is isoprene (Wolfe et al., 2016a), it is likely that the biogenic contribution to OH reactivity is even higher than indicated here. Contributions from

Deleted: x

Moved down [2]: With the exception of isoprene and monoterpenes, alkenes were not measured onboard the AML.

Formatted: Font:Italic

Moved up [1]: $k_{OH} = \sum_i k_{(X+OH)}[X]_i$ ... [2]

Deleted: To estimate the impact of anthropogenic alkenes on OH reactivity, we include observations from nearby TCEQ monitoring sites, Camp Bullis for UTSA and a site in Floresville co-located with the AML. These sites provide hourly observations of alkenes, including cis-2-butene, trans-2-butene, 1-pentene, cis-2-pentene, trans-2-pentene, ethene, propene, 1,3-butadiene, and 1-butene. Comparison of *alkanes* measured onboard the AML to those measured at the Camp Bullis TCEQ site shows only marginal agreement, suggesting that alkene concentrations used here might also differ between the SAFS and TCEQ sites. In any case, the inclusion or omission of these alkene observations from the TCEQ sites has almost no effect on the results. Alkenes contribute less than 1% of total reactivity at both UTSA and Floresville for morning and afternoon times, so we do not include them in our discussion below.
(4) ... [1]

Deleted: ... [3]

Deleted: x

Deleted: x

alkanes were unimportant at the UTSA site, 1% or less during both morning and afternoon, and contributed only 4-5% at Floresville.

The uncertainty in the isoprene measurements does not significantly alter the conclusions presented here. To bound the effect of this uncertainty, we adjusted the isoprene observations by ± 32% and recalculated the OH reactivity. This results in a range of 10.5 – 13.4 and 3.8 – 4.3 s^{-1} in total afternoon OH reactivity at UTSA and Floresville, respectively. NO_X remains the dominant contributor at UTSA in the morning. For the lower bound, isoprene contributes 49% of total OH reactivity at UTSA, by far the largest contributor to afternoon OH reactivity, and 23% at Floresville, making it second in importance to CO (25%).

Because of the large contribution of alkenes to OH reactivity at other Texas sites (Mao et al., 2010), it is necessary to make an estimate of their importance during SAFS. With the exception of isoprene and monoterpenes, alkenes were not measured onboard the AML and therefore have not been included in the above analysis. To estimate the impact of anthropogenic alkenes on OH reactivity, we include in our calculation of OH reactivity observations of alkenes made at nearby TCEQ monitoring sites, Camp Bullis for UTSA and a site in Floresville co-located with the AML. These sites provide hourly observations of cis-2-butene, trans-2-butene, 1-pentene, cis-2-pentene, trans-2-pentene, ethene, propene, 1,3-butadiene, and 1-butene. Alkene concentrations at the SAFS monitoring sites were assumed to be identical to those at the TCEQ monitoring sites and were interpolated to the ECHAMP time base. This assumption is likely more accurate for the Floresville site than for UTSA. A regression of hourly averaged *n*-pentane measured onboard the AML to that measured at the Camp Bullis TCEQ site has an r^2 of 0.3, even after maximizing the correlation using a lead-lag analysis. In addition, the maximum *n*-pentane concentrations at the Camp Bullis site are almost a factor of 2 higher than those seen at

Formatted: Indent: First line: 0.5"

Deleted: Anthropogenic alkenes have little impact on total OH reactivity at the AML measurement sites.

Moved (insertion) [2]

UTSA. Regressions of cyclohexane and benzene between the two sites show even lower r^2 values. On the other hand, a similar regression of n-pentane at the Floresville site has an r^2 of 0.83. Better agreement at Floresville is to be expected since the AML and TCEQ monitor were co-located. Total OH reactivity was then recalculated using the estimates of alkene concentrations. Alkenes contribute less than 1% of total reactivity at both UTSA and Floresville for morning and afternoon times.

4. Discussion and conclusions

We have presented observations of O_3, its precursors, and total observations of XO_2 at three sites in the San Antonio region. We also presented determinations of $P(O_3)$ calculated from measurements of total peroxy radicals. Median daytime $P(O_3)$ at UTSA was 4.1 ppbv hr^{-1}, compared to just over 1 ppbv hr^{-1} at the other two SAFS sites. Ozone production rates at UTSA were still far lower, however, than values observed during campaigns in Houston. Mazzuca et al. (2016) found median near surface gross $P(O_3)$ of about 10 ppbv hr^{-1} during the DISCOVER-AQ campaign in the summer of 2013, with values up to 140 ppbv hr^{-1} seen over the Houston shipping channel. These values are consistent with previous studies in the region (Sommariva et al., 2011). Higher concentrations of NO and larger production rates of RO_X were seen during DISCOVER-AQ than during SAFS, both of which could lead to higher $P(O_3)$.

During SAFS, ozone peaked at UTSA at 80 ppbv, with a median value of 47 ppbv, almost 20 ppbv higher than at the background site of Floresville, upwind of San Antonio. Along with higher O_3, the UTSA site also had larger $P(O_3)$, isoprene, NO, and XO_2 concentrations than upwind sites. Differences in $[O_3]$ between the up- and downwind sites could be the result of the effects of urban emissions on O_3 production, or they could result from daily variability, since simultaneous observations were not made at both sites and there are no permanent O_3

Formatted: Indent: First line: 0.5"

Deleted:

observations at Floresville. Figure S5 compares O_3 observations from the AML while at UTSA to those made by the University of Houston (UH), who measured O_3 continuously at UTSA during SAFS, and to observations from the TCEQ sites at Lake Calaveras, located upwind of downtown San Antonio (Fig. 2b), and Pecan Valley, situated in downtown San Antonio. Between 17 and 30 May, winds in the San Antonio region were primarily southeasterly (*i.e.* they travelled in the general direction from Lake Calaveras to UTSA, with downtown San Antonio in-between). During this period, there are both days where O_3 is almost identical at all sites and where O_3 is 20 ppbv higher at UTSA than at Lake Calaveras, suggesting significant O_3 production in the air as it travelled between the two sites. These results suggest that the 20 ppbv differences in median values between the UTSA and Floresville sites could be either the result of day-to-day variability, *in situ* O_3 production as the air travelled between the two sites, or a mixture of the two. Further observations of O_3 and its precursors in the region, including in downtown San Antonio, are needed to fully characterize the effects of the city on ozone production. In addition, future modeling studies will investigate the evolution of ozone production during this campaign.

A variety of methods were used to show that with the exception of early morning, when NO is high and XO_2 concentrations are low due to limited insolation, ozone production at the three SAFS sites is NO_X-limited. The relationship between $P(O_3)$ and NO was consistent at the three sites, although the lower $P(RO_X)$, NO, and VOC reactivity at Floresville and Corpus Christi led to overall lower ozone production rates as compared to UTSA. VOC-limited points comprised only 20% of total daytime observations and generally had $P(O_3)$ less than 5 ppbv hr^{-1} at UTSA and less than 2 ppbv hr^{-1} at the other two sites. This diurnal cycle is in agreement with observations made in Houston during the DISCOVER-AQ (Mazzuca et al., 2016) and SHARP

Deleted: 3

Deleted: both

Deleted:

Deleted:

Deleted: The

Deleted:

(Ren et al., 2013) campaigns. These results, however, are limited to the examined time period and location, but comparison to O_3 and NO levels at the Camp Bullis site suggests the observations at UTSA are typical for an area downwind of the San Antonio urban center. This is in contrast, however, to observations at the TCEQ Pecan Valley site which has not had an ozone exceedance day by either EPA standard since 2015 but regularly has MDA8 NO greater than 50 ppbv, significantly larger than the maximum 2-minute value of 4 ppbv seen at the UTSA site. Mixing ratios of O_X at Pecan Valley and Camp Bullis (Fig. 1) are essentially identical, suggesting that there is less O_3 titration downwind of central San Antonio than in the urban core. Given the higher [NO_X] in the urban core of San Antonio, $P(O_3)$ could be significantly different than at the UTSA site. Supporting this idea of variations in ozone production across the San Antonio region is the time series of O_3 at Pecan Valley, UTSA, and Lake Calaveras during SAFS (Fig. S5). Ozone concentrations are frequently lower at this site than at both UTSA and Lake Calaveras, despite its location downwind of Lake Calaveras.

OH reactivity at UTSA was found to be 12 s^{-1}, with the primary contributor being isoprene. While the overall magnitude of the reactivity was comparable to that observed and modeled during the TRAMP2006 campaign in Houston (Mao et al., 2010), the contributors to OH reactivity were found to be significantly different. Contributions from aromatics were negligible at UTSA while they were found to be 15% during TRAMP2006. In Houston, anthropogenic alkenes were found to be responsible for 20-30% of total reactivity, with biogenic VOCs making up less than 10%. Here, biogenic VOCs were responsible for 55% of total daytime reactivity, with alkenes making up less than 1%, although alkene values were based on estimates from a different site. We caution that this result cannot necessarily be extrapolated to other areas in the San Antonio region. Isoprene has a lifetime on the order of an hour, and the

Moved (insertion) [3]

Deleted: 3

Moved up [3]: Given the higher [NO_X] in the urban core of San Antonio, $P(O_3)$ could be significantly different than at the UTSA site.

high biogenic contribution to OH reactivity seen here could result from local influences. While there are trees throughout the San Antonio region, the results at UTSA cannot be extrapolated to areas with far less foliage without further observations. Other VOCs could comprise a larger fraction of total OH reactivity in less vegetated areas.

While the isoprene concentration at Floresville was significantly lower than at UTSA, it was still the dominant contributor to OH reactivity during the afternoon, although the total OH reactivity was a factor of 3 lower at this site (4 s^{-1}) than at UTSA. Schade and Roest (2016) found a significantly different OH reactivity profile at Floresville than described here, with alkanes accounting for approximately 70% of total OH reactivity, with biogenic VOCs contributing less than 5%. Observed isoprene at Floresville during SAFS was more than an order of magnitude larger than that reported in Schade and Roest (2016), with alkane concentrations consistent between the two studies. When the data used in Schade and Roest (2016) are subset to afternoon times and May through July, the contribution of isoprene to VOC reactivity increases to a median value of 38%, in agreement with the results presented here (Schade, personal communication). The differences between the two studies do suggest that there could be significant seasonal and diurnal variations in OH reactivity. Nevertheless, these results suggest that policies designed to limit O_3 production at the SAFS sites discussed here should initially focus primarily on NO_X reductions as the region is NO_X limited and the primary VOC contributor is biogenic. Further observations and analysis are need to determine whether this holds true in the urban core of downtown San Antonio.

5. Data Availability

Data from SAFS are maintained on a private server but are available upon request to the authors.

Deleted: a chemical environment at UTSA that differs from the rest of San Antonio

Deleted: .

Deleted: Further observations are needed to confirm that this is true for the entire region.

Deleted: They report statistics for yearly data of individual species concentrations from 2013 to 2014, so direct comparisons are difficult.

Deleted: Differences in reactivity could result from differences in biogenic emissions as well as in differences in anthropogenic emissions, as fossil fuel production in the Eagle Ford Shale region (outlined in Fig. 2) has declined recently.

6. Author Contributions

D.CA. and E.W wrote the manuscript. All authors discussed the results and commented on the manuscript. All authors also contributed to daily running of the AML. S.C.H. led the campaign. D.C.A., J.P, and E.C.W. measured XO_2. B.M.L. and W.B.K. contributed to the measurement of organic trace gases. J.R.R., T.I.Y., and S.C.H. led observations with TILDAS instruments as well as measurements of NO, NO_2, and O_3.

7. Competing Interests

The authors declare no competing interests.

8. Acknowledgements

The authors acknowledge support from NSF grants AGS-1443842 and AGS-1719918. In addition, this research was funded by a grant (project 17-032) from the Texas Air Quality Research Program (AQRP) at the University of Texas Austin through the Texas Emission Reduction Program (TERP) and the Texas Commission on Environmental Quality (TCEQ). The findings, opinions, and conclusions are the work of the authors and do not necessarily represent the findings, opinions, or conclusions of the AQRP or the TCEQ. The authors thank S. Hall and K. Ullmann of NCAR, J. Flynn of the University of Houston, D. Sullivan of the University of Texas at Austin, and R. Nadkarni and M. Estes of TCEQ for their contributions to the SAFS campaign and this paper.

Formatted: Font:12 pt

Formatted: Font:12 pt

Formatted: Font:12 pt

Formatted: Font:12 pt

9. References

Bell, M. L., Peng, R. D., and Dominici, F.: The exposure-response curve for ozone and risk of mortality and the adequacy of current ozone regulations, Environmental Health Perspectives, 114, 532-536, 10.1289/ehp.8816, 2006.

Bucsela, E. J., Krotkov, N. A., Celarier, E. A., Lamsal, L. N., Swartz, W. H., Bhartia, P. K., Boersma, K. F., Veefkind, J. P., Gleason, J. F., and Pickering, K. E.: A new stratospheric and tropospheric NO₂ retrieval algorithm for nadir-viewing satellite instruments: applications to OMI, Atmos. Meas. Tech., 6, 2607-2626, 10.5194/amt-6-2607-2013, 2013.

Choi, Y., and Souri, A. H.: Chemical condition and surface ozone in large cities of Texas during the last decade: Observational evidence from OMI, CAMS, and model analysis, Remote Sensing of Environment, 168, 90-101, 10.1016/j.rse.2015.06.026, 2015.

Cooper, O. R., Gao, R.-S., Tarasick, D., Leblanc, T., and Sweeney, C.: Long-term ozone trends at rural ozone monitoring sites across the United States, 1990-2010, Journal of Geophysical Research: Atmospheres, 117, n/a-n/a, 10.1029/2012jd018261, 2012.

Duncan, B. N., Yoshida, Y., Olson, J. R., Sillman, S., Martin, R. V., Lamsal, L., Hu, Y., Pickering, K. E., Retscher, C., Allen, D. J., and Crawford, J. H.: Application of OMI observations to a space-based indicator of NOx and VOC controls on surface ozone formation, Atmospheric Environment, 44, 2213-2223, 10.1016/j.atmosenv.2010.03.010, 2010.

Duncan, B. N., Lamsal, L. N., Thompson, A. M., Yoshida, Y., Lu, Z. F., Streets, D. G., Hurwitz, M. M., and Pickering, K. E.: A space-based, high-resolution view of notable changes in urban NOx pollution around the world (2005-2014), Journal of Geophysical Research-Atmospheres, 121, 976-996, 10.1002/2015jd024121, 2016.

EPA: National Ambient Air Quality Standards for Ozone, Federal Register, 80, 2015.

Faloona, I. C., Tan, D., Lesher, R. L., Hazen, N. L., Frame, C. L., SImpas, J. B., Harder, G., Martinez, M., Di Carlo, P., Ren, X., and Brune, W. H.: A Laser-induced Fluorescence Instrument for Detecting Tropospheric OH and HO2: Characteristics and Calibration, Journal of Atmospheric Chemistry, 47, 139-167, 2004.

González Abad, G., Liu, X., Chance, K., Wang, H., Kurosu, T. P., and Suleiman, R.: Updated Smithsonian Astrophysical Observatory Ozone Monitoring Instrument (SAO OMI) formaldehyde retrieval, Atmospheric Measurement Techniques, 8, 19-32, 10.5194/amt-8-19-2015, 2015.

He, H., Stehr, J. W., Hains, J. C., Krask, D. J., Doddridge, B. G., Vinnikov, K. Y., Canty, T. P., Hosley, K. M., Salawitch, R. J., Worden, H. M., and Dickerson, R. R.: Trends in emissions and concentrations of air pollutants in the lower troposphere in the Baltimore/Washington airshed from 1997 to 2011, Atmospheric Chemistry and Physics, 13, 7859-7874, 10.5194/acp-13-7859-2013, 2013.

Herndon, S. C., Jayne, J. T., Zahniser, M. S., Worsnop, D. R., Knighton, B., Alwine, E., Lamb, B. K., Zavala, M., Nelson, D. D., McManus, J. B., Shorter, J. H., Canagaratna, M. R., Onasch, T. B., and Kolb, C. E.: Characterization of urban pollutant emission fluxes and ambient concentration distributions using a

mobile laboratory with rapid response instrumentation, Faraday Discussions, 130, 327-339, 10.1039/b500411j, 2005.

Holton, J. R., Haynes, P. H., McIntyre, M. E., Douglass, A. R., Rood, R. B., and Pfister, L.: Stratosphere-Troposphere Exchange, Reviews of Geophysics, 33, 403-439, 1995.

Jerrett, M., Burnett, R. T., Pope, C. A., Ito, K., Thurston, G., Krewski, D., Shi, Y. L., Calle, E., and Thun, M.: Long-Term Ozone Exposure and Mortality, New England Journal of Medicine, 360, 1085-1095, 10.1056/NEJMoa0803894, 2009.

Kebabian, P. L., Herndon, S. C., and Freedman, A.: Detection of Nitrogen Dioxide by Cavity Attenuated Phase Shift Spectroscopy, Analytical Chemistry, 77, 724-728, 10.1029/, 2005.

Kebabian, P. L., Wood, E. C., Herndon, S. C., and Freedman, A.: A Practical Alternative to Chemiluminescence-Based Detection of Nitrogen Dioxide: Cavity Attenuated Phase Shift Spectroscopy, Environmental Science & Technology, 42, 6040-6045, 2008.

Kleinman, L. I.: LOW AND HIGH NOX TROPOSPHERIC PHOTOCHEMISTRY, Journal of Geophysical Research-Atmospheres, 99, 16831-16838, 10.1029/94jd01028, 1994.

Kleinman, L. I., Daum, P. H., Imre, D., Lee, Y. N., Nunnermacker, L. J., Springston, S. R., Weinstein-Lloyd, J., and Rudolph, J.: Ozone production rate and hydrocarbon reactivity in 5 urban areas: A cause of high ozone concentration in Houston, Geophysical Research Letters, 29, 105-101-105-104, 10.1029/2001gl014569, 2002.

Kleinman, L. I.: The dependence of tropospheric ozone production rate on ozone precursors, Atmospheric Environment, 39, 575-586, 10.1016/j.atmosenv.2004.08.047, 2005.

Krotkov, N. A., Lamsal, L. N., Celarier, E. A., Swartz, W. H., Marchenko, S. V., Bucsela, E. J., Chan, K. L., Wenig, M., and Zara, M.: The version 3 OMI NO2 standard product, Atmospheric Measurement Techniques, 10, 3133-3149, 10.5194/amt-10-3133-2017, 2017.

Kundu, S., Deming, B. L., Lew, M. M., Bottorff, B. P., Rickly, P., Stevens, P. S., Dusanter, S., Sklaveniti, S., Leonardis, T., Locoge, N., and Wood, E. C.: Peroxy Radical Measurements by Ethane – Nitric Oxide Chemical Amplification and Laser-Induced Fluorescence/Fluorescence Assay by Gas Expansion during the IRRONIC field campaign in a Forest in Indiana, Atmos. Chem. Phys. Discuss., 2019, 1-31, 10.5194/acp-2018-1359, 2019.

Lamarque, J. F., Hess, P., Emmons, L., Buja, L., Washington, W., and Granier, C.: Tropospheric ozone evolution between 1890 and 1990, Journal of Geophysical Research-Atmospheres, 110, 10.1029/2004jd005537, 2005.

Lamsal, L. N., Duncan, B. N., Yoshida, Y., Krotkov, N. A., Pickering, K. E., Streets, D. G., and Lu, Z. F.: U.S. NO2 trends (2005-2013): EPA Air Quality System (AQS) data versus improved observations from the Ozone Monitoring Instrument (OMI), Atmospheric Environment, 110, 130-143, 10.1016/j.atmosenv.2015.03.055, 2015.

Lee, B. H., Wood, E. C., Herndon, S. C., Lefer, B. L., Luke, W. T., Brune, W. H., Nelson, D. D., Zahniser, M. S., and Munger, J. W.: Urban measurements of atmospheric nitrous acid: A caveat on the interpretation of the HONO photostationary state, Journal of Geophysical Research: Atmospheres, 118, 12,274-212,281, 10.1002/2013jd020341, 2013.

880 Mao, J. Q., Ren, X., Chen, S., Brune, W. H., Chen, Z., Martinez, M., Harder, H., Lefer, B., Rappenglück,
881 B., Flynn, J., and Leuchner, M.: Atmospheric oxidation capacity in the summer of Houston 2006:
882 Comparison with summer measurements in other metropolitan studies, Atmospheric Environment, 44,
883 4107-4115, 10.1016/j.atmosenv.2009.01.013, 2010.

884 Mazzuca, G. M., Ren, X., Loughner, C. P., Estes, M., Crawford, J. H., Pickering, K. E., Weinheimer, A.
885 J., and Dickerson, R. R.: Ozone production and its sensitivity to NOx and VOCs: results from the
886 DISCOVER-AQ field experiment, Houston 2013, Atmospheric Chemistry and Physics, 16, 14463-14474,
887 10.5194/acp-16-14463-2016, 2016.

888 McManus, J. B., Zahniser, M. S., Nelson, D. D., Shorter, J. H., Herndon, S. C., Jervis, D., Agnese, M.,
889 McGovern, R., Yacovitch, T. I., and Roscioli, J. R.: Recent progress in laser-based trace gas instruments:
890 performance and noise analysis, Applied Physics B-Lasers and Optics, 119, 203-218, 10.1007/s00340-
891 015-6033-0, 2015.

892 Mihele, C. M., and Hastie, D. R.: Optimized operation and calibration procedures for radical amplifier-
893 type detectors, Journal of Atmospheric and Oceanic Technology, 17, 788-794, 10.1175/1520-
894 0426(2000)017<0788:Ooacpf>2.0.Co;2, 2000.

895 Orlando, J. J., and Tyndall, G. S.: Laboratory studies of organic peroxy radical chemistry: an overview
896 with emphasis on recent issues of atmospheric significance, Chemical Society Reviews, 41, 6294-6317,
897 10.1039/c2cs35166h, 2012.

898 Park, S. K., O'Neill, M. S., Vokonas, P. S., Sparrow, D., and Schwartz, J.: Effects of air pollution on heart
899 rate variability: The VA Normative Aging Study, Environmental Health Perspectives, 113, 304-309,
900 10.1289/ehp.7447, 2005.

901 Pollack, I. B., Ryerson, T. B., Trainer, M., Parrish, D. D., Andrews, A. E., Atlas, E. L., Blake, D. R.,
902 Brown, S. S., Commane, R., Daube, B. C., de Gouw, J. A., Dubé, W. P., Flynn, J., Frost, G. J., Gilman, J.
903 B., Grossberg, N., Holloway, J. S., Kofler, J., Kort, E. A., Kuster, W. C., Lang, P. M., Lefer, B., Lueb, R.
904 A., Neuman, J. A., Nowak, J. B., Novelli, P. C., Peischl, J., Perring, A. E., Roberts, J. M., Santoni, G.,
905 Schwarz, J. P., Spackman, J. R., Wagner, N. L., Warneke, C., Washenfelder, R. A., Wofsy, S. C., and
906 Xiang, B.: Airborne and ground-based observations of a weekend effect in ozone, precursors, and
907 oxidation products in the California South Coast Air Basin, Journal of Geophysical Research:
908 Atmospheres, 117, n/a-n/a, 10.1029/2011jd016772, 2012.

909 Pollmann, J., Helmig, D., Hueber, J., Tanner, D., and Tans, P. P.: Evaluation of solid adsorbent materials
910 for cryogen-free trapping - gas chromatographic analysis of atmospheric C2-C6 non-methane
911 hydrocarbons, Journal of Chromatography A, 1134, 1-15, 10.1016/j.chroma.2006.08.050, 2006.

912 Ren, X., van Duin, D., Cazorla, M., Chen, S., Mao, J., Zhang, L., Brune, W. H., Flynn, J. H., Grossberg,
913 N., Lefer, B. L., Rappenglück, B., Wong, K. W., Tsai, C., Stutz, J., Dibb, J. E., Thomas Jobson, B., Luke,
914 W. T., and Kelley, P.: Atmospheric oxidation chemistry and ozone production: Results from SHARP
915 2009 in Houston, Texas, Journal of Geophysical Research: Atmospheres, 118, 5770-5780,
916 10.1002/jgrd.50342, 2013.

917 Ring, A. M., Canty, T. P., Anderson, D. C., Vinciguerra, T. P., He, H., Goldberg, D. L., Ehrman, S. H.,
918 Dickerson, R. R., and Salawitch, R. J.: Evaluating commercial marine emissions and their role in air
919 quality policy using observations and the CMAQ model, Atmospheric Environment, 173, 96-107,
920 10.1016/j.atmosenv.2017.10.037, 2018.

Ryerson, T. B., Trainer, M., Angevine, W. M., Brock, C. A., Dissly, R. W., Fehsenfeld, F. C., Frost, G. J., Goldan, P. D., Holloway, J. S., Hubler, G., Jakoubek, R. O., Kuster, W. C., Neuman, J. A., Nicks, D. K., Parrish, D. D., Roberts, J. M., Sueper, D. T., Atlas, E. L., Donnelly, S. G., Flocke, F., Fried, A., Potter, W. T., Schauffler, S., Stroud, V., Weinheimer, A. J., Wert, B. P., Wiedinmyer, C., Alvarez, R. J., Banta, R. M., Darby, L. S., and Senff, C. J.: Effect of petrochemical industrial emissions of reactive alkenes and NOx on tropospheric ozone formation in Houston, Texas, Journal of Geophysical Research-Atmospheres, 108, 10.1029/2002jd003070, 2003.

Sanchez, J., Tanner, D. J., Chen, D., Huey, L. G., and Ng, N. L.: A new technique for the direct detection of HO₂ radicals using bromide chemical ionization mass spectrometry (Br-CIMS): initial characterization, Atmospheric Measurement Techniques, 9, 3851-3861, 10.5194/amt-9-3851-2016, 2016.

Sanders, S. P., Friedl, R. R., Abbatt, J. P. D., Barker, J. R., Burkholder, J. B., Golden, D. M., Kolb, C. E., Kurylo, M. J., Moortgat, G. K., Wine, P. H., R.E., H., and Orkin, V. L.: Chemical Kinetics and Photochemical Data for Use in Atmopsheric Studies, 2011.

Schade, G. W., and Roest, G.: Analysis of non-methane hydrocarbon data from a monitoring station affected by oil and gas development in the Eagle Ford shale, Texas, Elementa: Science of the Anthropocene, 4, 10.12952/journal.elementa.000096, 2016.

Schroeder, J. R., Crawford, J. H., Fried, A., Walega, J., Weinheimer, A., Wisthaler, A., Müller, M., Mikoviny, T., Chen, G., Shook, M., Blake, D. R., and Tonnesen, G. S.: New insights into the column CH2O/NO2 ratio as an indicator of near-surface ozone sensitivity, Journal of Geophysical Research: Atmospheres, 10.1002/2017jd026781, 2017.

Shetter, R. E., Junkermann, W., Swartz, W. H., Frost, G. J., Crawford, J. H., Lefer, B. L., Barrick, J. D., Hall, S. R., Hofzumahaus, A., Bais, A., Calvert, J. G., Cantrell, C. A., Madronich, S., Muller, M., Kraus, A., Monks, P. S., Edwards, G. D., McKenzie, R., Johnston, P., Schmitt, R., Griffioen, E., Krol, M., Kylling, A., Dickerson, R. R., Lloyd, S. A., Martin, T., Gardiner, B., Mayer, B., Pfister, G., Roth, E. P., Koepke, P., Ruggaber, A., Schwander, H., and van Weele, M.: Photolysis frequency of NO2: Measurement and modeling during the International Photolysis Frequency Measurement and Modeling Intercomparison (IPMMI), Journal of Geophysical Research-Atmospheres, 108, 10.1029/2002jd002932, 2003.

Silva, R. A., West, J. J., Zhang, Y., Anenberg, S. C., Lamarque, J.-F., Shindell, D. T., Collins, W. J., Dalsoren, S., Faluvegi, G., Folberth, G., Horowitz, L. W., Nagashima, T., Naik, V., Rumbold, S., Skeie, R., Sudo, K., Takemura, T., Bergmann, D., Cameron-Smith, P., Cionni, I., Doherty, R. M., Eyring, V., Josse, B., MacKenzie, I. A., Plummer, D., Righi, M., Stevenson, D. S., Strode, S., Szopa, S., and Zeng, G.: Global premature mortality due to anthropogenic outdoor air pollution and the contribution of past climate change, Environmental Research Letters, 8, 034005, 10.1088/1748-9326/8/3/034005, 2013.

Sommariva, R., Brown, S. S., Roberts, J. M., Brookes, D. M., Parker, A. E., Monks, P. S., Bates, T. S., Bon, D., de Gouw, J. A., Frost, G. J., Gilman, J. B., Goldan, P. D., Herndon, S. C., Kuster, W. C., Lerner, B. M., Osthoff, H. D., Tucker, S. C., Warneke, C., Williams, E. J., and Zahniser, M. S.: Ozone production in remote oceanic and industrial areas derived from ship based measurements of peroxy radicals during TexAQS 2006, Atmospheric Chemistry and Physics, 11, 2471-2485, 10.5194/acp-11-2471-2011, 2011.

Stark, H., Lerner, B. M., Schmitt, R., Jakoubek, R., Williams, E. J., Ryerson, T. B., Sueper, D. T., Parrish, D. D., and Fehsenfeld, F. C.: Atmospheric in situ measurement of nitrate radical (NO3) and other photolysis rates using spectroradiometry and filter radiometry, Journal of Geophysical Research-Atmospheres, 112, 10.1029/2006jd007578, 2007.

964 Thornton, J. A.: Ozone production rates as a function of NOx abundances and HOx production rates in
965 the Nashville urban plume, Journal of Geophysical Research, 107, 10.1029/2001jd000932, 2002.

966 Whalley, L. K., Stone, D., Dunmore, R., Hamilton, J., Hopkins, J. R., Lee, J. D., Lewis, A. C., Williams,
967 P., Kleffmann, J., Laufs, S., Woodward-Massey, R., and Heard, D. E.: Understanding in situ ozone
968 production in the summertime through radical observations and modelling studies during the Clean air for
969 London project (ClearfLo), Atmospheric Chemistry and Physics, 18, 2547-2571, 10.5194/acp-18-2547-
970 2018, 2018.

971 Wolfe, G. M., Kaiser, J., Hanisco, T. F., Keutsch, F. N., de Gouw, J. A., Gilman, J. B., Graus, M., Hatch,
972 C. D., Holloway, J., Horowitz, L. W., Lee, B. H., Lerner, B. M., Lopez-Hilifiker, F., Mao, J., Marvin, M.
973 R., Peischl, J., Pollack, I. B., Roberts, J. M., Ryerson, T. B., Thornton, J. A., Veres, P. R., and Warneke,
974 C.: Formaldehyde production from isoprene oxidation across NOx regimes, Atmospheric Chemistry and
975 Physics, 16, 2597-2610, 10.5194/acp-16-2597-2016, 2016a.

976 Wolfe, G. M., Marvin, M. R., Roberts, S. J., Travis, K. R., and Liao, J.: The Framework for 0-D
977 Atmospheric Modeling (F0AM) v3.1, Geosci. Model Dev., 9, 3309-3319, 10.5194/gmd-9-3309-2016,
978 2016b.

979 Wood, E. C., Deming, B. L., and Kundu, S.: Ethane-Based Chemical Amplification Measurement
980 Technique for Atmospheric Peroxy Radicals, Environmental Science & Technology Letters, 4, 15-19,
981 10.1021/acs.estlett.6b00438, 2017.
982

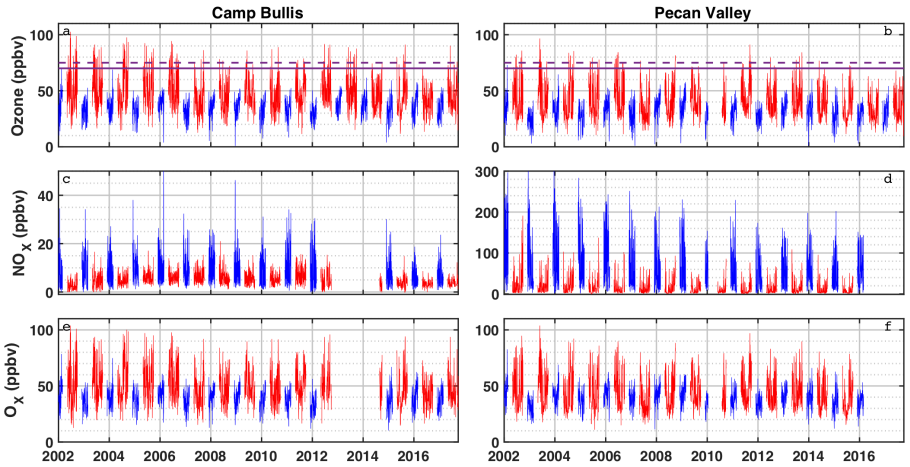

983

984 **Figure 1:** Time series of maximum daily average 8-hour (MDA8) O_3, NO_X, and O_X at the Camp
985 Bullis (**a**, **c**, **e**) and Pecan Valley (**b**, **d**, **f**) TCEQ sites for 2002 – 2017. Summer months (May –
986 September) are shown in red, and winter months (December – February) are shown in blue. MDA8
987 is calculated by determining the maximum value of a species from running 8 hour averages
988 throughout the day. The purple dashed and solid red lines represent the 2008 (75 ppbv) and 2015

(70 ppbv) O_3 standards respectively. Data were downloaded from www.tceq.texas.gov/goto/tamis.

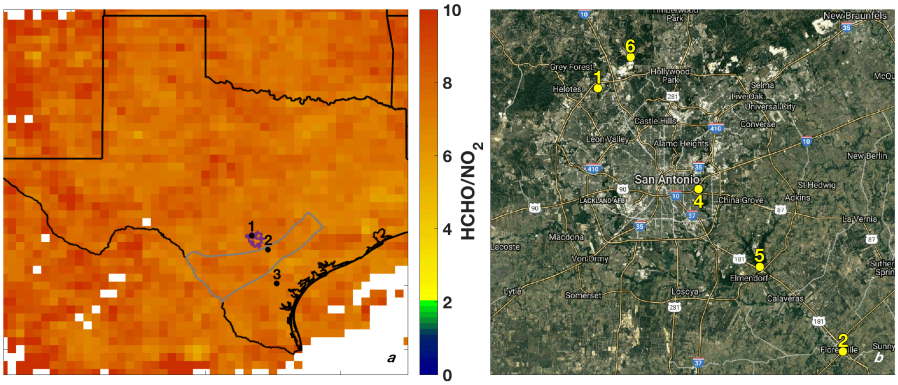

Figure 2: The sampling locations for the Aerodyne mobile laboratory are indicated: 1 – University of Texas San Antonio, 2 – Floresville, 3 – Lake Corpus Christi. The ratio of total column HCHO to tropospheric column NO_2 averaged over the months of May through July 2017 is also shown for grid boxes with 10 or more observations of both species over the indicated time period. The outlines of the Eagle Ford Shale (grey) play and San Antonio city limits (purple) are also shown for reference. (b) The major roadways and TCEQ monitoring stations (6: Camp Bullis, 4: Pecan Valley, 5: Calaveras Lake) in the San Antonio region used in this study are shown. The UTSA and Floresville SAFS sites are also shown for reference.

Deleted: is

Deleted: in grey

Deleted: A

Deleted: C

Deleted: D

Deleted: (B)

Deleted: is

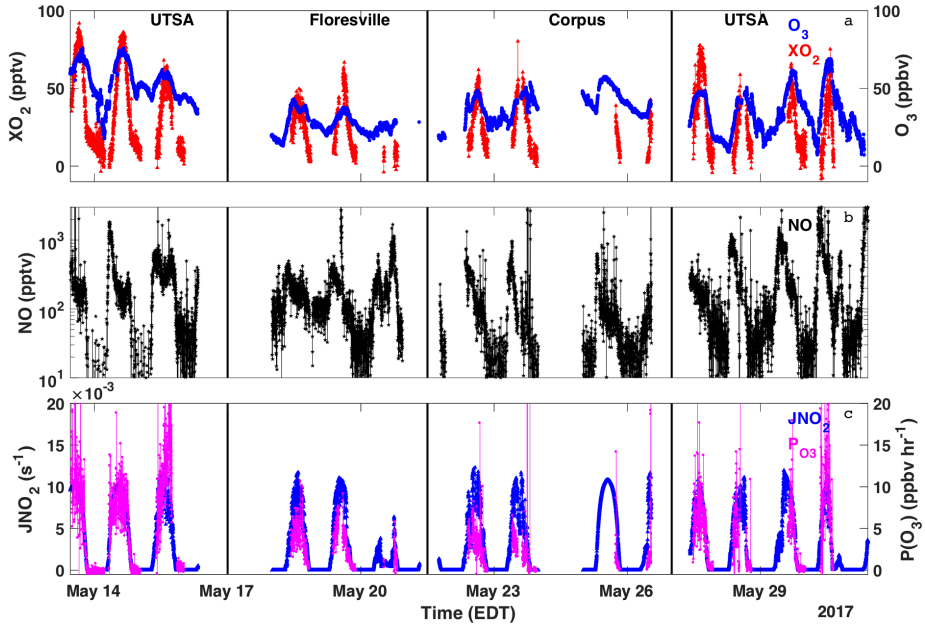

Figure 3: Time series of O_3 (blue circles), XO_2 (red triangles), NO (black stars), JNO_2 (blue triangles), and $P(O_3)$ (magenta circles) measured at all sites. All data are averaged over the XO_2 sampling period.

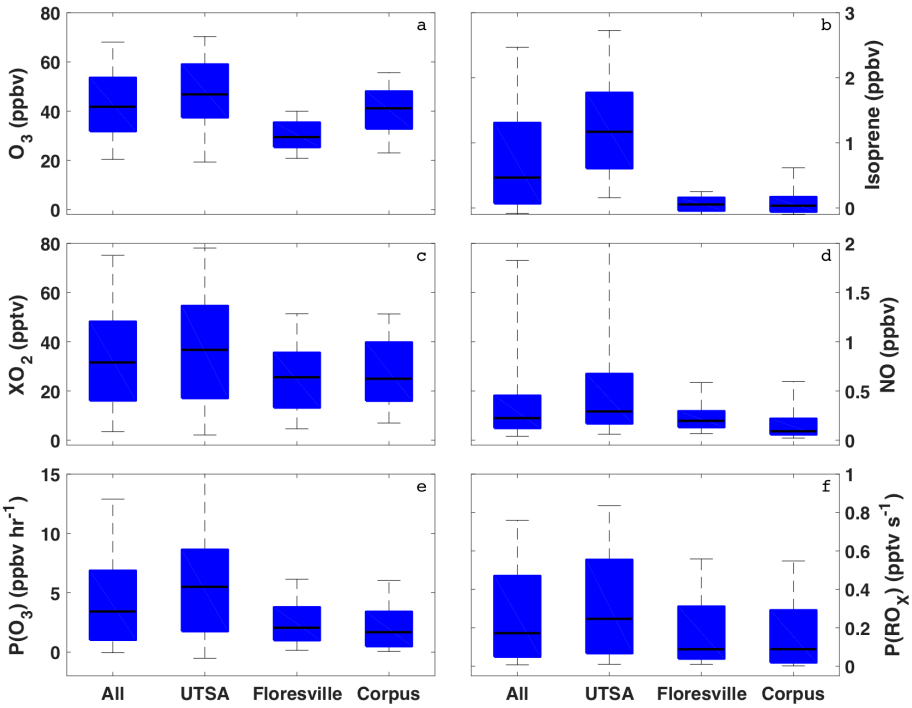

Figure 4: The distribution of O_3 (**a**), isoprene (**b**), XO_2 (**c**), NO (**d**), $P(O_3)$ (**e**), and $P(RO_X)$ (**f**) for all observations during SAFS taken between 07:00 and 20:00. The distribution for the entire campaign (All) as well as at the individual sites is shown. Medians are indicated by the black lines, and the 5th, 25th, 75th, and 95th percentiles are shown by the edges of the box and whiskers.

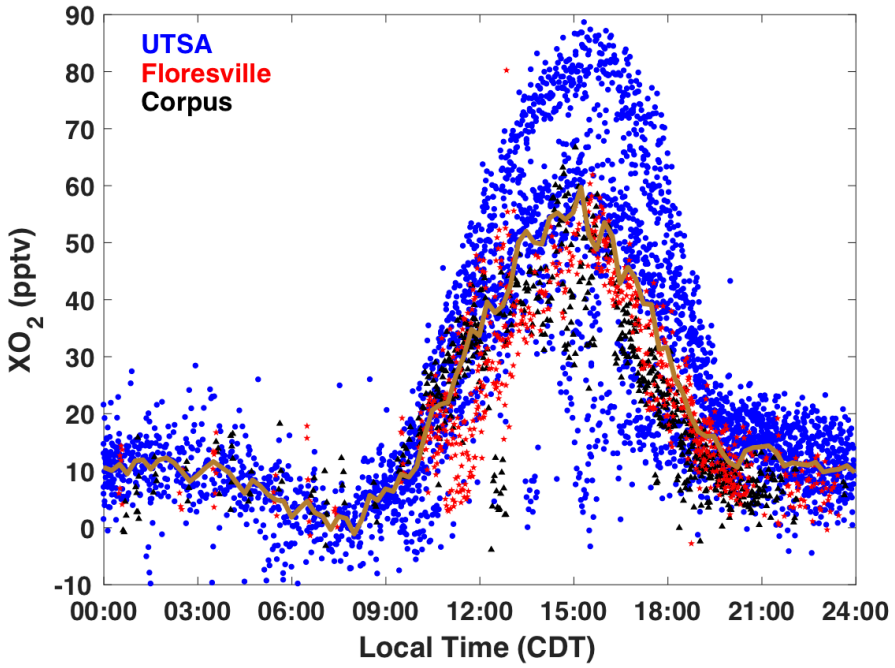

Figure 5: The diurnal profile of all 2 minute average XO_2 observations made during SAFS. Observations made at UTSA are shown in blue, Floresville, in red, and Corpus, in black. The median value for 15-minute time bins for observations at all sites is shown by the gold trace.

Formatted: Normal

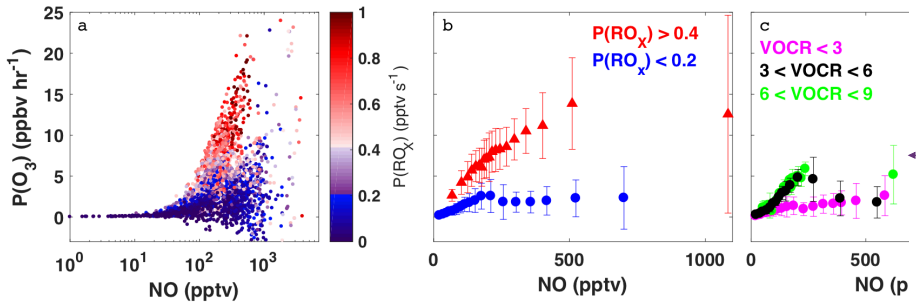

Figure 6: The variation of $P(O_3)$ with NO for all daytime observations (07:00 to 20:00) made during SAFS (**a**). Observations are colored by $P(RO_X)$. The same data as shown in panel (**a**) but sorted by $P(RO_X)$ are shown in panel (**b**). Observations with $P(RO_X)$ greater than 0.4 pptv s^{-1} are shown in red, while observations with $P(RO_X)$ less than 0.2 pptv s^{-1} are shown in blue. Data are separated into NO bins with an equal number of observations in bin. The mean value of each bin is shown, with the error bars showing one standard deviation. The subset of observations with $P(RO_X) < 0.2$ pptv s^{-1} are further separated into three categories: low VOC reactivity (VOCR < 3 s^{-1}; magenta), medium VOC reactivity (3 < VOCR < 6 s^{-1}; black), and high VOC reactivity (6 < VOCR < 9 s^{-1}; green) (**c**). As in panel (**b**) data are separated into NO bins with equal numbers of observations in each bin.

Formatted: Centered

Deleted: 5

Deleted: 15

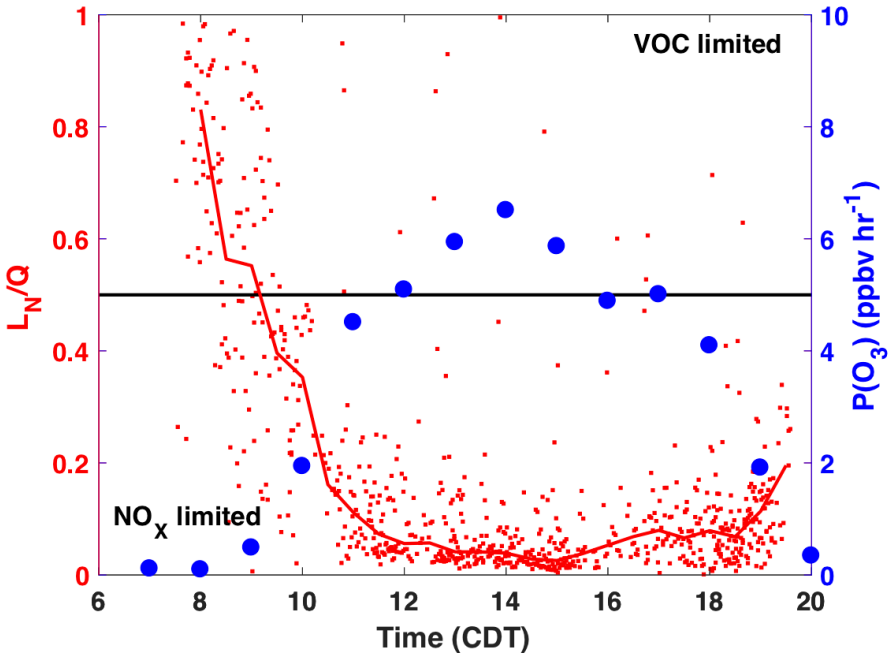

Figure 7: The diurnal profiles of L_N/Q calculated with the F0AM box model (red), and the median $P(O_3)$ in one hour time bins (blue). The median L_N/Q value for half hour bins is shown by the red line. Profiles are only for observations at UTSA. Points are calculated by $P(O_3)$ calculated from observations. The black line is approximately the separation between the NO_X- and VOC-limited regimes.

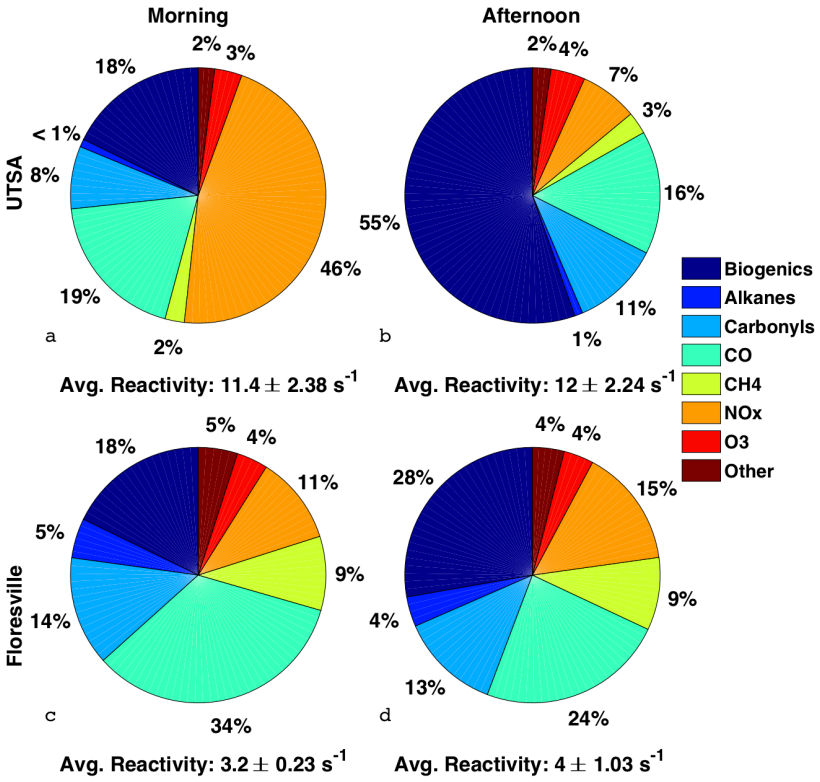

Figure 8: The distribution of the various contributors to the overall OH reactivity for the UTSA (13 -16 May) and Floresville (17 – 19 May) sites are shown for both the morning, times between 7:00 and 11:00, and afternoon, times between 13:00 and 20:00. The average OH reactivity (±1σ) is also shown.

Page 22: [1] Deleted	Microsoft Office User	1/11/19 1:54:00 PM

To estimate the impact of anthropogenic alkenes on OH reactivity, we include observations from nearby TCEQ monitoring sites, Camp Bullis for UTSA and a site in Floresville co-located with the AML. These sites provide hourly observations of alkenes, including cis-2-butene, trans-2-butene, 1-pentene, cis-2-pentene, trans-2-pentene, ethene, propene, 1,3-butadiene, and 1-butene. Comparison of *alkanes* measured onboard the AML to those measured at the Camp Bullis TCEQ site shows only marginal agreement, suggesting that alkene concentrations used here might also differ between the SAFS and TCEQ sites. In any case, the inclusion or omission of these alkene observations from the TCEQ sites has almost no effect on the results. Alkenes contribute less than 1% of total reactivity at both UTSA and Floresville for morning and afternoon times, so we do not include them in our discussion below.

$$k_{OH} = \sum_i k_{(X+OH)}[X]_i \quad (4)$$

Page 22: [2] Moved to page 4 (Move #1)	Microsoft Office User	1/2/19 3:40:00 PM

$$k_{OH} = \sum_i k_{(X+OH)}[X]_i \quad (4)$$

Page 22: [3] Deleted	Microsoft Office User	1/2/19 3:38:00 PM